Advances in Science and Technology Research Journal

Advances in Science and Technology Research Journal, 2025, 19(6), 41–69
https://doi.org/10.12913/22998624/202784
ISSN 2299-8624, License CC-BY 4.0

Received: 2025.02.08
Accepted: 2025.04.15
Published: 2025.05.01

A review of the state-of-the-art in improving piezoelectric properties

Ali N. Al-Obiedy[1*], Ali H. Al-Helli[2]

[1] Department of Mechanical Engineering, College of Engineering, Al-Nahrain University Al-Jadriya, Baghdad Governorate, Iraq
[2] Unmanned Aerial Vehicle (UAV) Eng. Dep., College of Engineering, Al-Nahrain University, Baghdad, Iraq
* Corresponding author's e-mail: st.ali.n.odaa@ced.nahrainuniv.edu.iq

ABSTRACT

This review will present a collection of previous research studies in the field of enhanced piezoelectric properties. At first, an introduction will be provided about the field of energy, methods of harvesting energy, the field of employing piezoelectricity, and also the concept of piezoelectricity to convert mechanical energy into electrical energy when used as a sensor. It can be employed as an actuator that can convert electrical energy into mechanical energy. This paper will provide an overview of techniques for enhancing the characteristics of piezoelectric materials. There are many of these methods, such as composite and hybrid materials, partial size, shape, and dimension, compressibility, lamination, 3D printed piezoelectric, coating, functional grid materials, hybrid systems, and more. For each method, different materials were used to prepare the piezoelectric. These materials can be broken down into several groups, such as smart materials that have piezoelectric effects, shape memory effects, and pyroelectric effects; reinforcement materials as multi-walled carbon nanotubes (MWCNT), carbon fiber-reinforced polymer (CFRP), or glass fiber-reinforced polymer (GFRP); matrix materials as UV-curable resin, and polydimethylsiloxane (PDMS); materials that help with the distribution process as N,N-dimethylformamide (DMF); and electrode materials as copper, platinum, and graphene. Additionally, the size of the added materials was defined, as most are nanomaterials. We will display the hybrid system, which is multifunctional. It is considered an important aspect of future development. In this part, different effects are combined into one application. For example, the smart scaffold combines the piezoelectric and shape memory effects. The real benefit of the research is to make the material's properties work better in general, and piezoelectricity works better in particular. These improvements can be done by studying each method on its own and then trying to combine some improvement methods in future research to make piezoelectricity work better and make it useful in more situations.

Keywords: piezoelectric, 3d printer, enhancement methods, composite or hybrid material, energy harvesting.

INTRODUCTION

Recently, demand for energy has increased tremendously due to the advent of various advanced technologies, and hence researchers are trying to solve this energy crisis by harvesting energy from different ambient sources [1, 2]. Energy harvesting is defined as capturing minute amounts of energy from one or more of the surrounding energy sources, accumulating them, and storing them for later use. It is also referred to as power harvesting or energy scavenging [3]. Energy harvesters can reduce the planet's consumption of nonrenewable energy and alleviate the pollution caused by traditional batteries [4]. In the viewpoint of energy conversion, humans have already utilized energy harvesting technology in the form of windmills [5–7], geothermal energy [8–11], solar energy [12–14], watermills [15–18], biomass from plants [19–22], magnetic [23–26], and mechanical vibration [27–31]. The energy derived from natural sources, known as renewable energy, has emerged as a future power source due to the limitations of fossil fuels and the instability of nuclear power, such as the Fukushima nuclear crisis. Renewable energy harvesting plants generate kW or MW-level power, which is classified as macro energy harvesting technology. In contrast, microtechnology for energy harvesting focuses on alternatives to conventional batteries. This technology is based on sources like mechanical vibration, mechanical stress and strain, thermal energy from furnaces, heaters, and friction sources, sunlight or room light, the human body, and chemical or biological sources, which can generate mW or μW-level power [32]. The rapid advancement of mobile electronic technologies and artificial intelligence necessitates the ongoing increase of battery energy density. On the other hand, traditional batteries have limited energy storage capacity [3], short life cycles [33–35], and low efficiency. However, the emergence of renewable clean energy and its storage may provide a solution to the energy challenges in the future years. Although existing green energy sources can efficiently power electronic devices, they are challenging to apply to microelectronic devices with power on the scale of mW or μW due to their demanding usage conditions and significant power production [36, 37]. As a result of these factors, mechanical vibration energy has become a preferred energy source for microelectronic systems. Furthermore, mechanical energy sources are diverse: mechanical impacts, vibration waves, water flow or raindrops, vehicle transportation, body movements, blood circulation, heartbeat, breathing, and respiratory movements. The mechanical energy gathered might be utilized immediately or stored in a battery for later use. [1] Since piezoelectric materials can convert mechanical vibration into electrical energy with a basic structure, piezoelectric energy harvesting has gained attention as a self-power source for wireless sensor network systems [32, 38]. The efficiency of energy harvesting applications can increase via hybridization with other generators [39]. This design approach is represented by integrating piezoelectric with triboelectric [40], thermal [41], and electrostatic nanogenerators [42]. Piezoelectric energy harvesting technologies are expected to usher in an era of self-powered autonomous operation in various fields, including aeronautics, healthcare, wireless data transmission, civil engineering, the automotive industry, environmental monitoring, robotics [1], transportation, aerial applications, smart systems, microfluidics, biomedical, wearable and implantable electronics, tissue regeneration [43], monitoring the marine environment, safeguarding maritime rights and interests, building a smart ocean [44], sensors, actuators, interdigital transducers, and structural health monitoring [2].

The published review of research in the field of piezoelectricity looks at the materials and applications and tries to explain how piezoelectricity works [1, 2, 32, 43, 45–49]. This study, on the other hand, will look at the ways to improve the properties of piezoelectricity and show how to make it work better by using more than one method at the same time to get the right properties. We will also explain the methods of preparing and manufacturing piezoelectric materials, starting with piezoelectric materials, through mixing components and the process of fabricating samples. We will also highlight the most important points extracted from the study and review of previous research.

PIEZOELECTRIC CONCEPT

The piezoelectric effect was discovered by the Curie brothers in 1880 [50]. Briscoe and Dunn [51] defined piezoelectricity as "electric charge that accumulates in response to applied mechanical stress in materials that have non-Centro symmetric crystal structures" while Erturk and Inman [52] defined piezoelectricity as "a form of coupling between the mechanical and electrical behaviors of ceramics and crystals belonging to certain classes". The Greek origin of the word "piezoelectricity" is "squeeze or press" [42], which refers to the property of the piezoelectric materials to generate an electric field when a mechanical force is applied [53], as illustrated in Figure 1, A piezoelectric crystal is placed between two plate electrodes. When a force is applied to the plates, a stress will be produced in the crystal and a corresponding deformation. With certain crystals, this deformation will produce a potential difference at the surface of the crystal, and the effect is called the piezoelectric effect [54, 55]. The piezoelectric effect is divided into two phenomena: the direct piezoelectric effect and the converse piezoelectric effect [52]. The property of some materials to generate an electric field when a strain is applied (direct piezoelectric effect) [50]. The converse or inverse piezoelectric effect was mathematically deduced from the principles of thermodynamics a year later by Lippmann [56], and it states that a piezoelectric material will deform if an electric

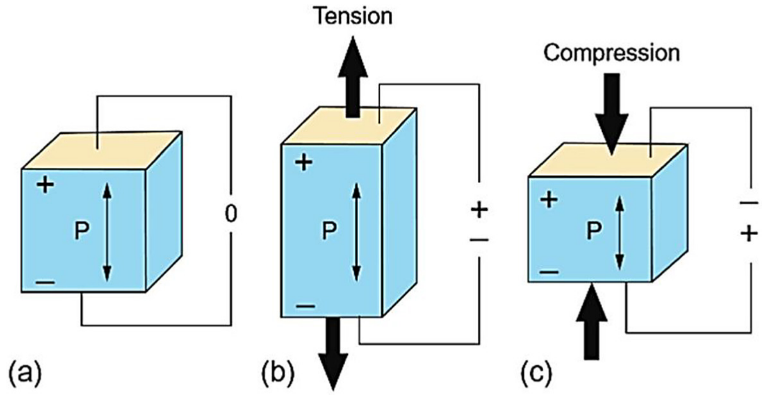

Figure 1. Schematic diagram of piezoelectric effect [58]

field is applied to it [53]. These two effects coexist in a piezoelectric material; therefore, ignoring the presence of one effect in an application would be thermodynamically inconsistent [57]. The electrical behavior of piezoelectric materials can be described using Hooke's law [51]. The induced charge on the crystal is proportional to the impressed force and is given by [54, 55]:

$$Q = d \cdot F \tag{1}$$

where: Q is electric charge generated (Coulombs), F is applied force (Newtons), and the proportionality constant d is called the piezoelectric constant. The output voltage of the crystal is given by:

$$E = g \cdot t \cdot p \tag{2}$$

where: t is the crystal thickness (meters), p is the impressed pressure (MPa), and g is called voltage sensitivity and is given by:

$$g = d / \varepsilon \tag{3}$$

where: d is the piezoelectric constant (C/N) and ε is the permittivity of the material (F/m).

METHODS USED TO IMPROVE PROPERTIES OF PIEZOELECTRIC

The published research is grouped by the method used to improve the properties. These methods include composite and hybrid materials, partial size, shape and dimension, compressibility, lamination, 3D printed piezoelectric, coating, functional grid materials, and hybrid systems. For each method, there is a summary of the materials used, partial size, electrode, preparation method, auxiliary and additional materials, tests, and some research results.

Composite material

Zhang et al.'s research from 2021 tries to manufacture flexible piezoelectric films as illustrated in Figure 2 using the solution casting and blade coating method, which includes incorporated lead zirconate titanate $Pb(Zr,Ti)O_3$ (PZT) ceramic nanomaterials and modified PZT by tetradecylphosphonic acid (TDPA) into the polyvinylidene fluoride-co-trifluoroethylene (PVDF-TrFE)

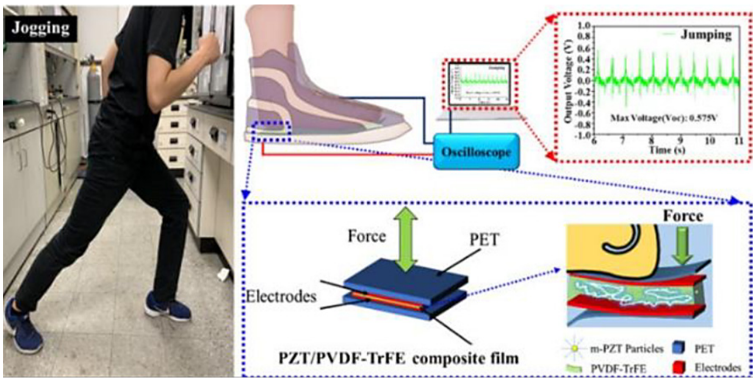

Figure 2. Design concept of PZT/PVDF-TrFE composite film and schematic diagram of the piezoelectric shoe application process [4]

copolymer matrix polymer for studying piezoelectric properties, as well as studying the best conditions for the annealing and polarization process. The results indicated that the improvement percentage for voltage output was 74.9% for M-PZT and 1.8% for PZT compared to samples without additions, while the best conditions for annealing and polarization were T = 140 °C, V = 4000 V, and t = 120 min [4]. Similarly, within the same investigation, Chao Zhang et al. (2021) investigated the development of film piezoelectric materials using PVDF as the polymer matrix and PZT as the piezoelectric filler. To enhance dispersion, they incorporated UP-105 titanate coupling reagent-modified PZT (M-PZT). The manufacturing process involved two methods: solution and extrusion casting. The materials were investigated for the tensile test, dielectric, ferroelectric, and piezoelectric properties, as well as the breakdown strength. The results indicated that the films prepared by extrusion casting have improved properties in terms of density, dielectric constant, breakdown strength, and piezoelectric coefficient [59]. Further exploring surface modification strategies, Ipsita Chinya et al. (2017) investigated the effect of surface modification on zinc ferrite (ZF) ceramic by PEG-6000 dispersion in PVDF polymer to manufacture flexible nanocomposite films by the solution casting method for optimization of maximum dielectric, ferroelectric, and piezoelectric performance. This composite exhibited 18 VOC AC touch sensing performance [60]. In contrast, adopting a different approach, Abhishek et al. (2018) reported the addition of Sodium Niobate ($NaNbO_3$) nanorods to PVDF polymer to manufacture thin film piezoelectric by the solution casting method as illustrated in Figure 3. A series of microstructural tests were performed, including XRD, FTIR, and polarization, in addition to examining piezoelectric response, dielectric properties, and energy harvesting performance. The results showed that $NaNbO_3$ nanorods not only facilitate the alignment of dipoles in PVDF but also increase the piezoelectric properties of the nanocomposite due to the inherent piezoelectric property of $NaNbO_3$ nanorods [61]. Expanding upon these studies, Sankar Ganesh et. al. (2017) studied the incorporation of bismuth ferrite ($BiFeO_3$ - BFO) ceramic into polydimethylsiloxane (PDMS) polymer at 50 wt.% and produced a flexible piezoelectric sandwich composed of graphene/$BiFeO_3$-PDMS/graphene, as illustrated in Figure 4. The results showed that the output voltage was 0.4 V by a normal pressure finger from a human hand [62]. In continuation of this work, Xiaohu Ren et. al. (2016) used the same materials and manufacturing method as illustrated in Figure 5 with different addition ratios from 10 to 40 wt.% and with aluminum (Al) electrodes. The result showed that the voltage was 3 V as the same procedure mentioned before [63]. Finally, concluding these investigations, Feifei Wang et. al. (2015) aimed to fabricate flexible piezoelectric from barium titanate ($BaTiO_3$) nanorods incorporated into polydimethylsiloxane (PDMS). The results showed that the voltage generation was 0.45 V [64]. For a comprehensive comparison of the materials, particle sizes, additive percentages, and fabrication methods discussed in these summaries, refer to Table 1.

Hybrid materials

Initially, Mehdi et al. [2022] aims to manufacture hybrid mixture piezoelectric films using the solution casting method, which includes

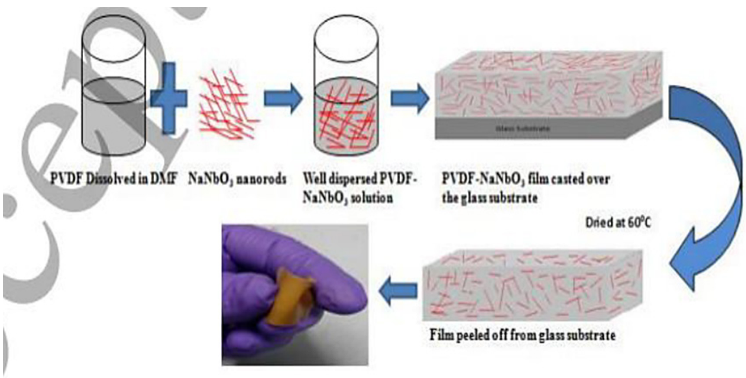

Figure 3. Schematic diagram representation for the synthesis of flexible PVDF-$NaNbO_3$ nanocomposite films [61]

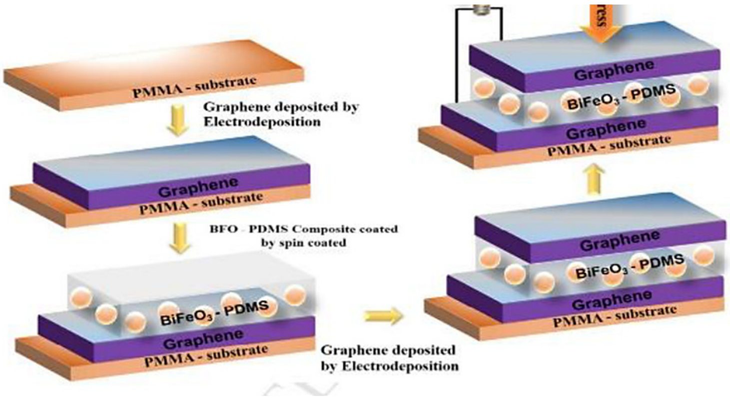

Figure 4. Schematic illustration of the sandwich structure of G/BFO-PDMS/G along with pressure direction [62]

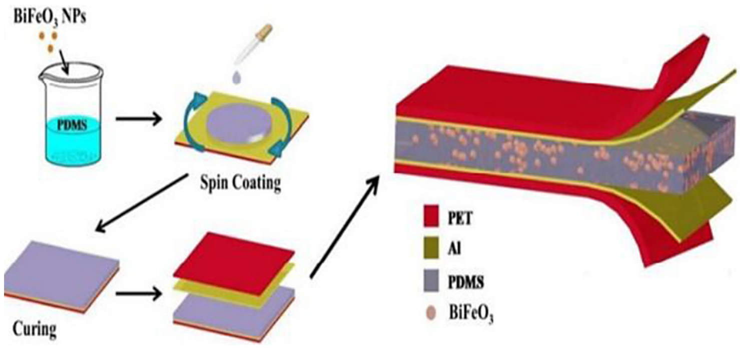

Figure 5. Schematic diagrams of the PNG fabricating process [63]

incorporated potassium sodium niobate (KNN) and multi-walled carbon nanotubes (MWCNTs), respectively, into the PVDF matrix polymer for studying microstructure, thermal, and piezoelectric properties. Through the results of the research, which showed that with the addition of KNN only to matrix enhancement, the properties of piezoelectric increased with an increased add ratio percentage until the height value, which was at 80 wt.%, and with the addition of MWCNT enhancement, the properties of piezoelectric increased to a percentage of 0.5 wt.%, and then decreased with an increase in the MWCNT add ratio. The enhancement was 78% and 57% at 0.5MWCNTs-80KNN-PVDF for the piezoelectric constant (d_{33}) and piezoelectric voltage constant (g_{33}) compared with the composite mixture 80KNN-PVDF, respectively [67]. Building upon this research, Satya Ranjan et. al. (2020) investigated the same materials but different particle forms of reinforcement materials, where carbon nanotubes (CNTs) and potassium sodium niobate nanorods were used. The incorporation of 0.1% CNTs into the PVDF/KNN composite enhanced the output voltage by 93.6% compared to without incorporation. In fact, the addition of CNTs led to a higher β-fraction and created a conducting path in the nanofiller-loaded polymer jet, which resulted in enhanced mechanical stretching of the electrospun fibers [68]. In the case of changing the second filler additive from MWCNT to Silicon Carbide (SIC) and changing the manufacturing method from traditional solution casting to hot-pressing as indicated in the Vajihe et. al. research, we notice that d_{33} decreased by 40% for the comparison between the best results, which were 50 and 30.5 pC/N for 0.5MWCNTs-80KNN-PVDF and 1SIC-80KNN-PVDF, respectively [69]. Extending the scope of material modifications, Kohei et al. (2022) included epoxy polymer as a matrix material, with the addition of KNN as a first filler reinforcement material, in addition to using the glass fiber-reinforced polymer (GFRP) as a secondary reinforcement material, as illustrated in Figure 6, to strengthen the mechanical and piezoelectric properties. The aim of the research is to study the mechanical and piezoelectric properties. The manufacturing method was the traditional solution casting. Through the research results, which showed an improvement in bending strength and elastic modulus in the length of about 4 times and 2 times, respectively, compared

Table 1. Summary of materials, particle size, enhancement methods, additive percentages, and fabrication approaches for piezoelectric composite materials

No.	Year	Materials						Methods Enhancement	Add. %	Ref.
		Polymer matrix materials	Additive materials	Particle size	Electrode	Additive layer	Modified materials			
1.	2022	PVDF-TrFE	PZT	800 nm	Electrode	PET	No	Heat treatment annealing and polarization +Composite material + simple doctor blade coating method	5, 10–50 wt.%	[4]
			Modified PZT By acid				TDPA	Heat treatment annealing and polarization + Composite material and modified by (TDPA)		
2.	2019	PVDF	Sodium Niobate (NaNbO3) nanorods	Nano size	Al	No	DMF	Composite material Without any treatment and additional processes	0–15 wt.%	[61]
3.	2017	PVDF	Zinc ferrite (ZF)	50 nm	Silver paste	No	PEG – 6000 and DMF	Solution casting method composite materials after casting hot pressured used	0–12 wt.%	[60]
			Modified Zinc ferrite (ZF)							
4.	2017	PDMS Not have piezoelectric effect	$BiFeO_3$ (BFO) Ceramic	Nano particles	Graphene	PMMA layer For flexiable	Chloroform	annealed Nano powder Spine coated Composite material Multilayer	50 wt.%	[62]
5.	2016	PDMS	BiFeO3	Nano particles	AL	PET layer For flexiable	Curing agent	spin-casted Composite material Multilayer	10, 20, 30, 40 wt.%	[63]
6.	2021	PVDF	no	1 µm	Silver		No	Without addition	5–45 wt.%	[59]
			PZT				UP-105 titanate coupling reagent	Composite material solvent casting		
			PZT					Composite material extrusion method		
7.	2015	Polydimethylsiloxane (PDMS)	Barium Titanate ($BaTiO_3$)	Nano rods diameters ~100–200 nm and grain size ~40 nm	Platinum	Silicon	No	Composite material	Undefined	[64]
8.	2018	PVDF-TrFE	MWCNT	Nano tube	Au	Silicon rubber	DMF	Electro spinning	0.2 wt.%	[65]
9.	2015	PVDF	Barium titanate BaTiO3	Nano size	Above AL and bottom Ni	Layer	Coupling agent	spin-coated Composite material	40 wt.%	[66]

to the control samples (KNN-epoxy), this means that the samples can now withstand a higher force, which enables them to be used in wider applications. This was proven by the damped flexural vibration energy harvesting test, as the samples without the GFRP failed. While the piezoelectric constant (d_{33}) for GFRP-KNN-epoxy was less than half the value of KNN-epoxy [70]. Finally, concluding this review, Huidrom et al. (2017) investigate the incorporation of $NaNbO_3$ (sodium niobate) and RGO (reduced graphene oxide) into PVDF, as illustrated in Figure 7, using traditional solution casting to manufacture film piezoelectric. Through the research results, we note that the resulting voltage improved by approximately 187% for the haybird mixture compared to the samples without addition [71]. For a comprehensive comparison of the materials, particle sizes, additive percentages, and fabrication methods discussed in these summaries, refer to Table 2.

Particle size and dimension

To begin with, Xiaoteng Chen et. al. (2022) incorporated $BaTiO_3$ with submicron particle sizes of 200 nm, 500 nm, and 600 nm into prepared

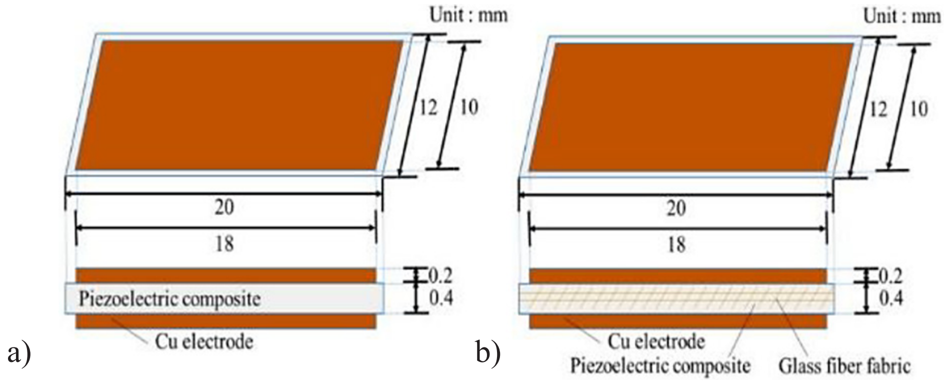

Figure 6. Schematic diagram of the piezoelectric composite samples (a) without and (b) with glass fibers [70]

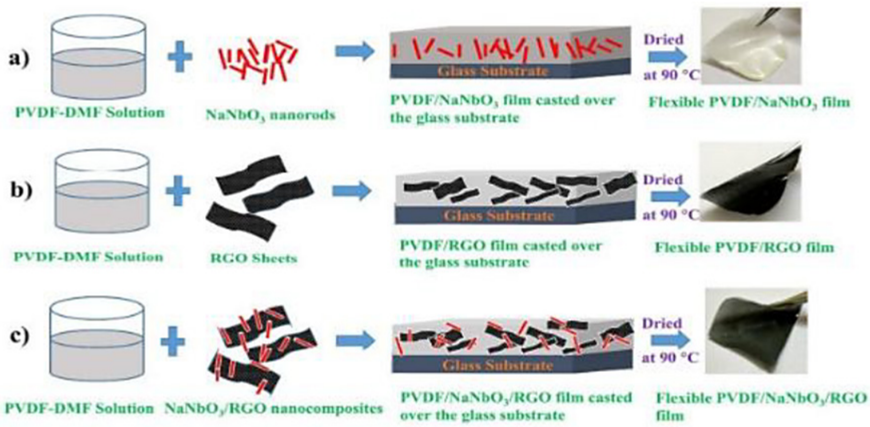

Figure 7. Schematic diagram showing the synthesis of the nanocomposite films [71]

UV resin (50 vol% HDDA and 50 vol% PEGDA) to fabricate dense piezoelectric by DLP 3D printer as illustrated in Figure 8. The rheological, photopolymerization behaviors, density, grain size, piezoelectric, and dielectric properties were investigated. Through the results that showed that the viscosity and the cure depth of the mixture were affected by the particle size, such that the viscosity decreases and the cure depth increases with an increase in the added particle size. While the relationship between piezoelectric coefficient and dielectric constant and particle size is a direct relationship, as they increase with the increase in the particle size of the added powder [73]. Expanding on the role of 3D printing in piezoelectric material fabrication, Renteria (2019) dealt with the use of different types of 3D printers (freeze-form extrusion fabrication (FEF)) to manufacture $BaTiO_3$ ceramic piezoelectric samples, as illustrated in Figures 9 and 10 that explain the stages of preparing the paste solution and 3D printer with samples. The aim of the research was to study the effect of particle size on the properties of the material. The results indicated that the relationship between the particle size and the density, dielectric constant, and piezoelectric coefficient was an inverse relationship; as the particle size increases, the values of properties increase [74]. Building upon this concept, the same researchers presented a second study on the integration of two different particle sizes of $BaTiO_3$ powder (100 nm and 400 nm) with a solution binder to fabricate dense piezoelectric samples by past extrusion with a 3D printer. A 50–50% vol. bimodal particle distribution achieved the highest packing density and a piezoelectric coefficient of 350 pC/N, which is a 40% improvement over using 100% vol. from 100 nm $BaTiO_3$ alone [75]. In a related investigation, Jia-Wun Li et al. (2020) explore the effects of particle dimensions on the crystalline structure and piezoelectric properties, where carbon was added in its three dimensions to the matrix (zero-dimensional (0D) carbon black (CB), one-dimensional (1D) carbon nanotubes (CNT-COOH), and two-dimensional (2D) graphene

Table 2. Summary of materials, particle size, enhancement methods, additive percentages, and fabrication approaches for piezoelectric hybrid materials

No.	Year	Materials						Methods Enhancement	Add. %	Ref.
		Polymer matrix materials	Additive materials	Particle size	Electrode	Additive layer	Modified materials			
1.	2022	PVDF	KNN Modified by DMF	Nano size	Silver paste	No	DMF	Hybrid material Solution casting method	50, 60, 70, and 80 wt.%	[67]
			KNN MWCNTs						KNN (50, 60, 70, and 80 wt.%), CNT (0, 0.25, 0.5, 0.75, and 1 wt. %)	
2.	2022	Two type of Epoxy (Bisphenol F and ST12)	KNN	Nano size	Cu tape	Teflon mold	No	Hybrid material Solution casting two layers from glass cloth	32 vol %	[70]
			KNN-glass fiber fabric							
3.	2021	PVDF	KNN	Nano size	Un defined	No	Ethanol for mixing	Hybrid material + hot compression molding	60–80 % wt.%	[69]
			KNN +SiC						60–70 % + SiC (0.5, 1 ,1.5) wt.%	
4.	2017	PVDF	no	Nano size	Copper	No	DMF	Solution Casting as dropped	1 g PVDF + 50 mg RGO / 100 mg NaNbO3 / 100 mg NaNbO3 + RGO	[71]
			RGO							
			NaNbO3							
			$NaNbO_3$ + RGO							
5.	2017	PDMS	$BaTiO_3$ + MWCNT	Nano fiber	Aluminum foil	No	Curing agent	Solution Casting	10 – 50 wt.% for $BaTiO_3$ and 0 – 5 wt.% for MWCNT	[72]
				10–15 nm, length of 10–20 μm						
6.	2020	PVDF	KNN + CNT	Nano rods	Al tape	Polypropylene (PP) tape	Dimethylformamide (DMF) and Acetone	Electro Spinning	3 wt.% for KNN and 0–0.5 wt.% for CNT	[68]

oxide (GO)), and to improve the spread, distribution, and prevention of agglomerations inside the matrix, a polymer dispersion was added: styrene-maleic anhydride copolymer (SMAz) and polyoxyalkylene amine (M1000). Post-processes included annealing and polarization treatments that were needed to transform the α-phase into the β-phase responsible for piezoresponse, as illustrated in Figure 11. The best result was obtained using modified CNT, which increased the β-phase content in PVDF-TrFE and piezoelectric coefficient by 17% and 34%, respectively [76]. Furthering this exploration, a study by Bharathi Ponraj et. al. (2016), which discusses the effect of particle size on the properties. The incorporation of KNN fillers in PVDF at both nanometer and micron scales above 10 vol% to manufacture piezoelectric samples by the hot-pressing method. The results showed that incorporation at both scales above 10 vol% resulted in the formation of a polar β-form of PVDF. The dielectric properties were better when using nanoscale than microscale at 40 vol%, and the opposite is true if the percentage increases to 70 vol% with respect to the piezoelectric coefficient (d_{33}), as the results show that the nano is not responsive [77]. For a comprehensive comparison of the materials, particle sizes, additive percentages, and fabrication methods discussed in these summaries, refer to Table 3.

Elastic compressibility effect

To start with, a study by Jianguo Sun et. al. (2021) achieves an enhancement in the piezoelectric response by increasing the elastic compressibility of balsa wood through a facile, green, and sustainable fungal decay pretreatment. Figure

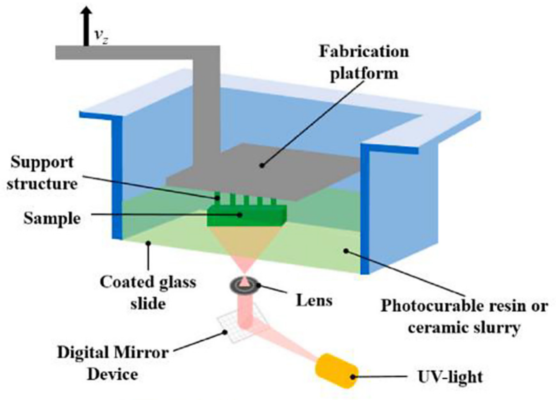

Figure 8. Manufacturing principles of DLP [73]

12 displays the difference between native wood that hasn't been treated and decayed wood that has been treated. It shows that the treated wood is easier to compress, as shown by the research results, which showed that the response value went up by 55 times [78]. In the same way, Jianguo Sun (2020) also investigates the same principle but another method, where a simple delignification process was used, which led to an enhanced piezoelectric response of 85% compared with native wood [79].

Lamination techniques

In the past few years (2019–2023), a group of researchers studied the effect of piezoelectric and mechanical properties of lamination piezoelectric film (KNN-epoxy) by using layers of carbon fiber-reinforced polymers (CFRPs) because of their excellent mechanical properties and use as electrodes. Initially, a study by Yaonan Yu et al. (2023) manufactured a piezoelectric film by the blade coating method as illustrated in Figure 13, then used two upper layers and two lower layers from CFRPs. The results showed an enhancement in bending strength and, therefore, an increase in the resulting voltage generation,

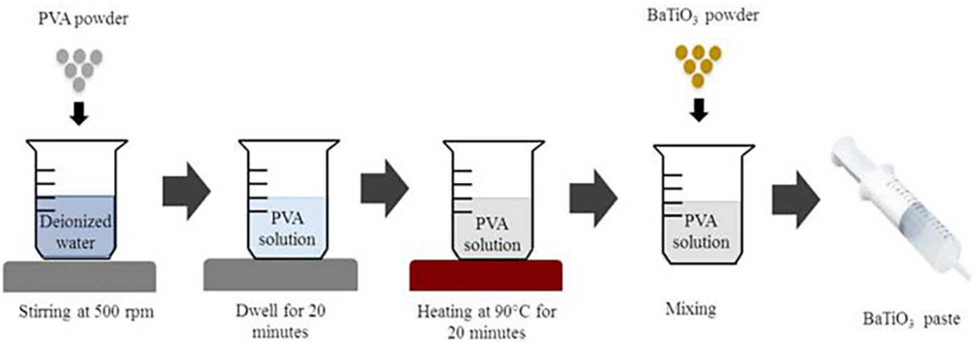

Figure 9. Schematic procedure for BTO/PVA aqueous paste [74]

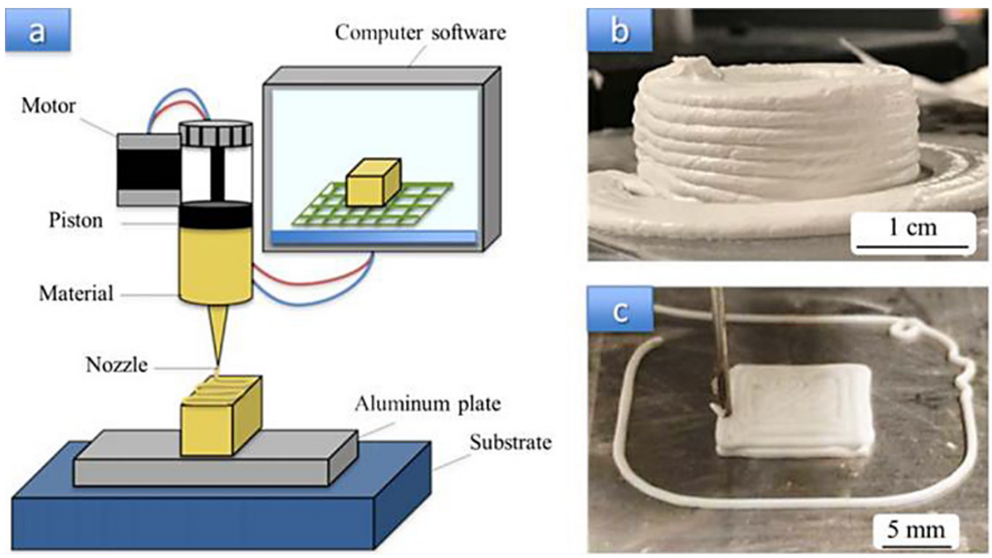

Figure 10. (a) Structure of 3D printing machine used for paste extrusion, (b) 3D printed cylinder structure, (c) 3D printing process of a square structure [74]

Figure 11. The effect of temperature annealing process on the appearance of piezoelectric film [76]

Table 3. Summary material, percentage, and methods Enhancement used to fabricate piezoelectric for Particle size and dimension

No.	Year	Materials						Methods Enhancement	Add. %	Ref.
		Polymer matrix materials	Additive materials	Particle size	Electrode	Additive layer	Modified materials			
1.	2022	Prepared UV resin (50 vol% HDDA and 50 vol% PEGDA)	$BaTiO_3$	200 nm	Coated by conductive silver	No	Dispersant BYK	DLP 3D printer Post-process debinding and sintering process	40 vol%	[73]
				500 nm						
				600 mm						
2.	2019	Binder (13wt. % PVA + deionized water)	$BaTiO_3$	100 nm	Conductive silver paint	No	No	FEF 3D printer Post-process debinding and sintering process	70 wt.%	[74]
				300 nm						
				500 nm						
3.	2021	Binder (13wt. % PVA + PAA deionized water)	$BaTiO_3$	100 nm + 400 nm	Conductive silver paint	No	No	Past extruding 3D printer Post-process debinding and sintering process	70 wt.%	[75]
4.	2020	PVDF-TrFE	No additive	Nano size	Silver glue	PET	Styrene-maleic anhydride copolymer (smaz) and polyoxyalkylene amine (M1000) + Methyl ethyl ketone (MEK)	Solution and wet coated	no	[76]
			(0D) carbon black (OCB)	40 nm				Heat treatment annealing Polarization +Composite material + solution and wet coated	0.1 0.5 1 3 5 wt.%	
			(1D) modified carbon nanotubes (CNT–COOH)	Diameter 10–20 nm						
			Two-dimensional (2D) graphene oxide (GO)	550 nm						
5.	2016	PVDF	KNN ceramic	Nanosize	Silver Coated	No	Acetone medium	Composite material Hot pressing (powder mixing and pressing)	10–40 vol%	[77]
				Microsize					10–70 vol%	

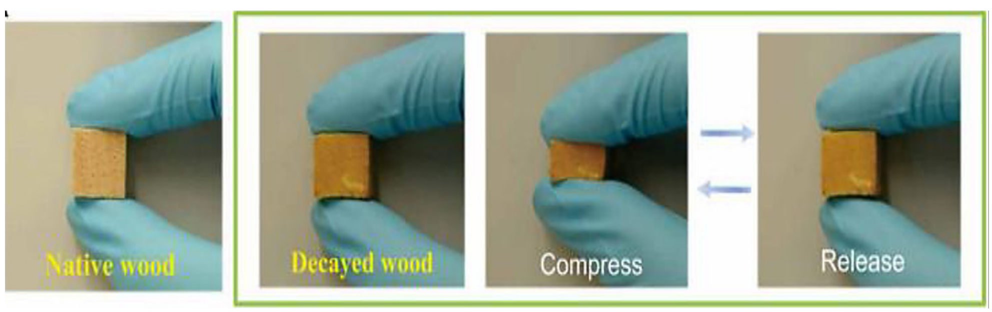

Figure 12. Photographs of the decayed wood showing its higher and reversible compressibility compared to native wood [78]

which was 6 times longer for CFRP-KNN-epoxy compared with piezoelectric without lamination KNN-epoxy. Increasing strength allows the use of piezoelectric in applications that require the use of materials with high strength. Therefore, this technology has increased the extent of the use of piezoelectrics [80]. In the same vein, in 2021, the same researchers used four layers of upper and two layers of lower as illustrated in Figure 14 to study the energy harvesting by bending technique; the results showed the voltage generation was 0.51 mV but a decrease in piezoelectric constant by 29.8% [81]. Furthermore, (2020) used two layers of upper and lower, as illustrated in Figure 15, to study the energy harvesting by impact and bending vibration techniques, and the results indicated that they have 0.8 μW/cm³ and 4 nW/cm³, respectively, for impact and bending tests but a decrease in piezoelectric constant by 26.5% [82]. In the same year, a study was published by Hiroki Kurita et. al. on the same concept of the work, which used KNN and BTO for comparing and adding individually to epoxy resin to fabricate piezoelectric samples by the solution casting method, then lamination by CFRP. The maximum stress and flexural modulus of KNN-epoxy-CFRP lamination were approximately 5–10% larger than those of BTO-epoxy-CFRP lamination [83]. In addition, Fumio Narita et. al. (2019) aimed to fabricate hybrid lamination consisting of a copper (Cu) electrode tape consisting of one upper and one lower layer and GFRP consisting of two upper and lower layers opposite orientation as illustrated in Figure

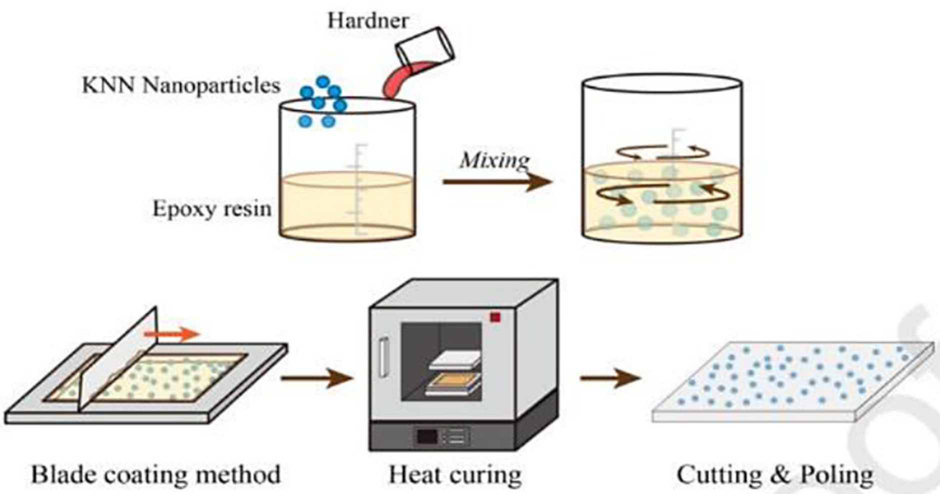

Figure 13. Schematic for the fabrication of KNN-nanoparticle-filled epoxy (KNN–EP) plate [80]

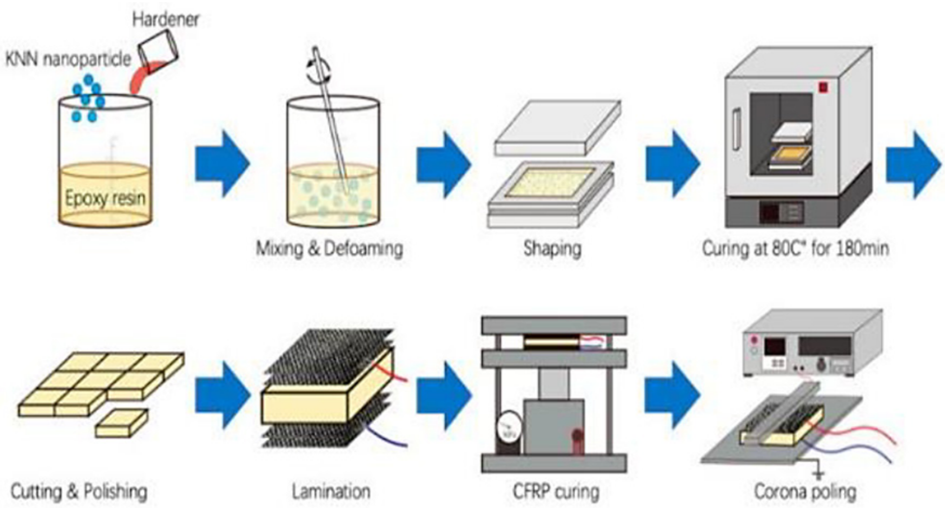

Figure 14. Schematic for the complete fabrication process of piezoelectric composite specimens [81]

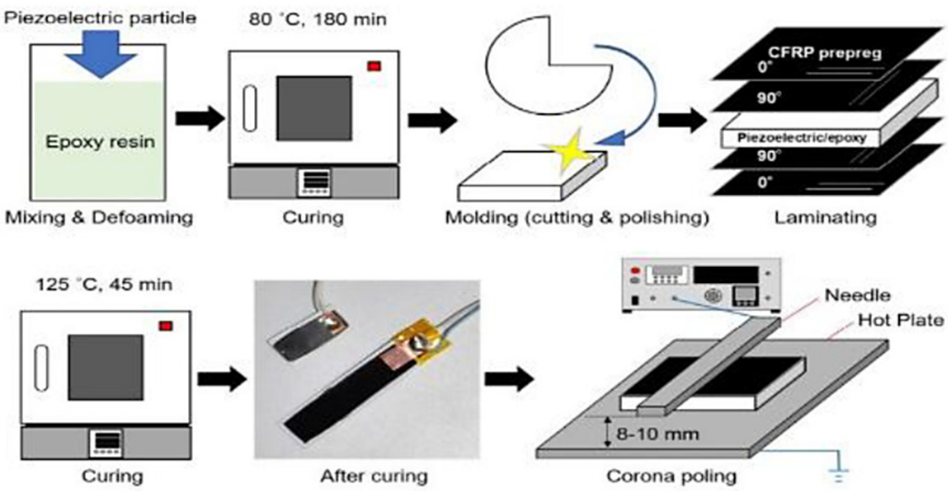

Figure 15. Schematic for the fabrication of KNN piezo-resin/CFRP composite material [82]

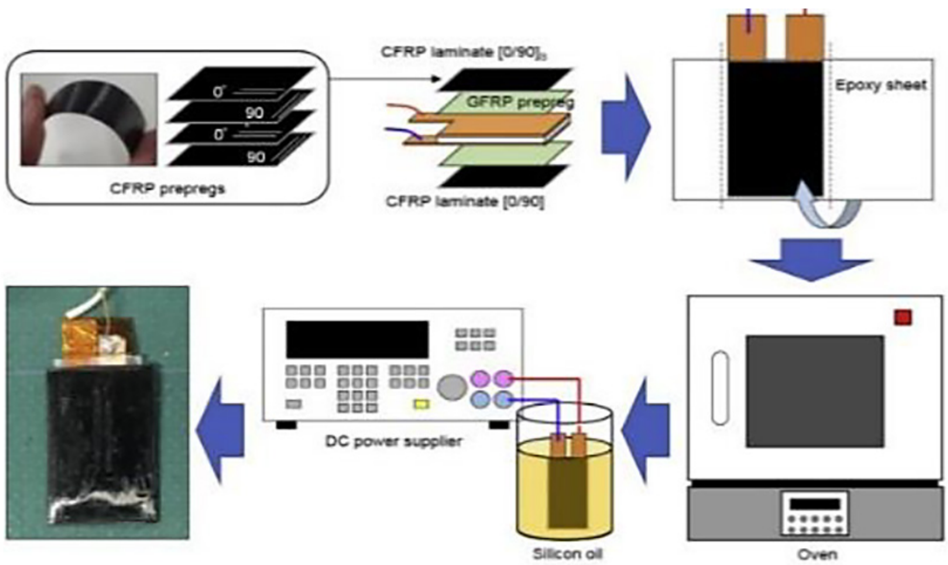

Figure 16. Schematic for the fabrication of piezoelectric hybrid CFRP composite material [84]

16 for studying the energy harvesting by impact technique, from the results that showed the voltage generation was 140 mV for lamination KNN-epoxy and 100 mV for lamination Barium Titanate ($BaTiO_3$)-epoxy[84]. Finally, CAM MINH et. al. (2010) aimed to fabricate multiple layers of different materials, such as copper electrode, carbon epoxy, and glass epoxy, layered onto a ceramic piezoelectric wafer (PZT), as illustrated in Figure 17. The maximum voltage generation was 2.56 V for the configuration of PCGE-A [85]. For a comprehensive comparison of the materials, particle sizes, additive percentages, and fabrication methods discussed in these summaries, refer to Table 4.

3D printed piezoelectric

Mold forming, mixing, and dicing-filing techniques are the main preparation methods for piezoelectric composite structures in the conventional fabrication process. However, these techniques are limited in fabricating shapes with complex structures. With the rapid development of additive manufacturing (AM), many research fields have applied AM technology to produce functional materials with various geometric shapes [86]. In the past few years (2020–2024), a group of researchers has employed the piezoelectric effect in applications that require the fabrication and manufacturing of complex shapes, such as scaffolds used in bone regrowth and

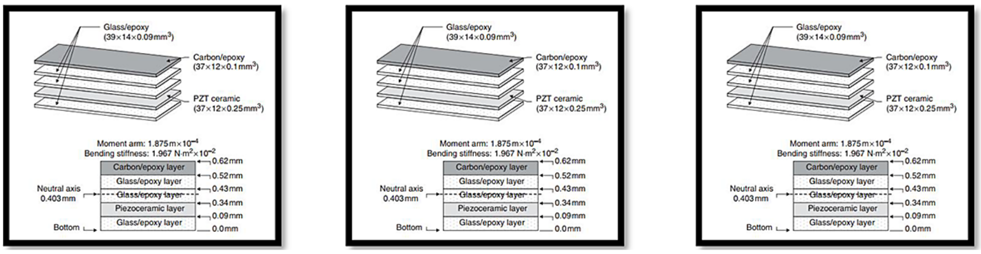

Figure 17. Geometry and position of the neutral axis of PCGE Types [85]

Table 4. Summary material, percentage, and methods Enhancement used to fabricate piezoelectric for Lamination method

No.	Year	Materials						Methods Enhancement	Add. %	Ref.
		Polymer matrix materials	Additive materials	Particle size	Electrode	Additive layer	Modified materials			
1.	2021	Bisphenol F epoxy resin	KNN	Nano size		Without	Hardener	4 upper and 2 lower layer Lamination + 2 method of poling	30 vol.%	[81]
			KNN		CFRP	CFRP prepregs				
2.	2023	Bisphenol F epoxy resin	KNN	Nano size		Without	Hardener	2 upper and 2 lower layer Lamination + 2 method of poling	25%, 30%, and 35%	[80]
			KNN		CFRP	CFRP prepregs				
3.	2020	Bisphenol-F epoxy resin	KNN	880 nm	Au-coated	Without	Hardener ST-12	2 up and 2 lower layer Lamination	30 vol.%	[82]
			KNN		CFRP	CFRP prepregs				
4.	2019	Epoxy (EP106N)	KNN	Nano size	Cu	CFRP prepregs	No	2 up and 2 lower layer from CFRP 2 layer (1 top and 1 lower) from Cu layer hybrid Lamination	35 vol.%	[84]
		Epoxy (EP106N)	$BaTiO_3$	Nano size	Cu	CFRP prepregs	No	2 up and 2 lower layer from CFRP 2 layer (1 top and 1 lower) from Cu layer hybrid Lamination		
5.	2010	PZT		Ceramic wafer	copper	Carbon/epoxy + glass/epoxy	No	Multilayer method By Different materials	no	[85]
6.	2020	Bisphenol-F epoxy resin	KNN	Nano size	Au	Without	Hardener	Lamination GFRP 0 CFRP 90 CFRP	30 vol.%	[83]
			KNN			CFRP GFRP				
			$BaTiO_3$			Without				
			$BaTiO_3$			CFRP GFRP				

fusion. To enhance the functional efficiency of scaffolds, which is done by incorporating smart piezoelectric materials into scaffolds that convert passive scaffolds into active and smart scaffolds with the complex shape manufactured by using a 3D printer. To begin with, Giovanna et. al. (2024) studied the effect of adding $BaTiO_3$ in nano size (< 3.0 µm) to the polyhydroxybutyrate (PHB) matrix in different weight ratios (5–20 wt.%) fabricated by using a Deposition Modeling (FDM) 3D printer, as illustrated in Figure 18. The morphological, thermal, biodegradation, mechanical, piezoelectric, and dielectric properties of the nanocomposites were studied. The results showed that increasing the percentage of added $BaTiO_3$ material, piezoelectric coefficients (d31), dielectric constant (ε_r), and piezoelectric voltage constant (g_{31}) increased, reaching the highest value at the highest percentage added, which was 20 wt.%, as follows: 37.46 pm/V, 6.29, and 0.67 V.m/N, with the figure of merit 25.2. The mechanical properties results showed that increasing the compression stress and modulus of elasticity approximated by 8.9 and 33%, while for tensile stress and elongation strain, the decrease was approximately 21% and 62%. [87]. In the same

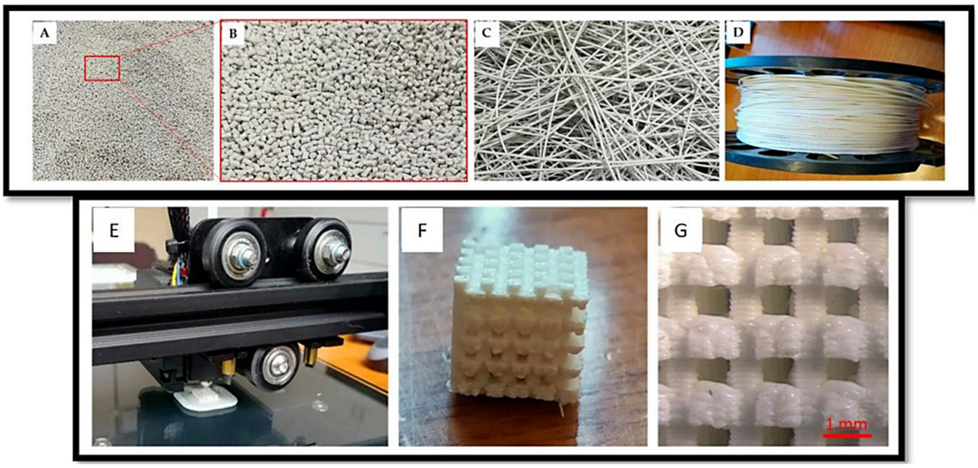

Figure 18. Photographs showing $BaTiO_3$/PHB 5/95 (w/w%) nano composite production: (A,B) pellets, (C,D) extruded filament, (E) printer sample by 3D printer,(F,G) sample

year, Rishikesh et. al. studied the effect of adding boron nitride nanotubes (BNNTs) at 2 wt.% to the mixed polymer matrix consisting of varied percentages of PVDF (20–40 wt.%) and UV resin 3D printer, where the aim was to fabricate piezoelectric samples by stereolithography 3D printer (LCD), as illustrated in Figure 19, and investigate the structural, thermal, rheological, mechanical, and piezoelectric properties. The results demonstrate the successful micro-scale printability. Additionally, it indicated that incorporating BNNTs into the polymer matrix enhanced the fraction of the β phase (F(B)), piezoelectric coefficient (d_{33}), dielectric constant (ε_r), piezoelectric voltage coefficient (g_{33}), and voltage output (V_0) as follows: 8, 66, 43, 16, and 50%, while the elastic modulus and hardness decrease by 62 and 25%, and the viscosity increased by 50% and temperature melting by 16% [88]. In 2021, Samuel E. Hall et al.'s research paper was about the direct writing (paste extrusion) fabrication of piezoelectrics from PZT mixed with water and post-processed sintered, as illustrated in Figure 20, then compared with the traditional fabrication method (die pressing method). A group of tests on viscosities, yield stresses, stability, density, and piezoelectric properties was performed on the samples. The results indicated that the two method values are close to equal for densities, piezoelectric coefficient, and dielectric constant, where the results d_{33}, ε_r, g_{33}, and FOM were 675, 4100, 0.0186, and 12.66, respectively [89]. Additionally, in the same year, Anton et. al. investigated methods for managing high additive concentrations of up to 70 wt.% and studied the effect of particle size (micro, submacro, and nano) on printability by incorporating $BaTiO_3$ into the SG15 UV resin LCD-SLA 3D printer. The steps

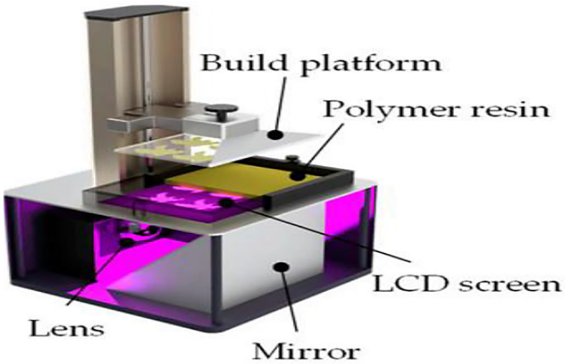

Figure 19. LCD 3D printing setup [88]

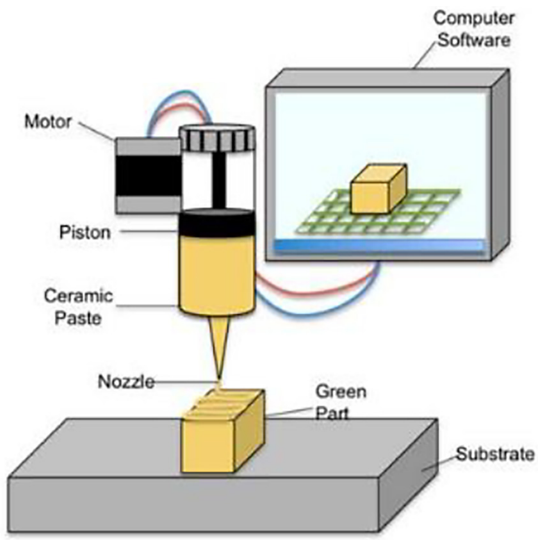

Figure 20. Schematic of Printrbot Simple Metal with paste-loaded syringe, plunged by a stepper motor-driven piston [89]

of the printing process are clearly illustrated in Figure 21. Investigates the structural, thermal, rheological, and piezoelectric properties. The results indicated that the viscosity of the liquid mixture increased with decreased particle size; the height value at the nanoscale was 400,000 MPa s. Moreover, the dielectric constant (ε_r), piezoelectric coefficient (d_{33}), and loss tangent (tan δ) were 1965, 200 (pC/N), and 1.7% (pC/N), respectively [90]. Furthermore, Emmanouela et. al. in the same year mention previous studies. Employ the 3D printing capability to form complex shapes with the hybrid principle using four mixing materials to increase the functional efficiency of a scaffold called scaffold multifunctional. It consists of poly(lactic acid) (PLA) as a matrix polymer mixture with another polymer, polycaprolactone (PCL), to increase its flexibility and decrease its brittleness. As for filler addition, two materials were used: the first $BaTiO_3$, which has a piezoelectric effect to benefit from this effect to increase the growth of bone defects, and the hydroxypyrite (HA) material, which has bioactivity for increasing strength adhesion to its bone surroundings. The working samples consisted of the following (PLA, PLA-PCL, PLA-PCL-0-20 wt.% HA, and 0-20 wt.% $BaTiO_3$) and used 3D printer filaments (FDM) to fabricate test samples. Through the results, it was indicated that the mixture had piezoelectric properties close to bone, an increase in elongation by 30%, and a decrease in strength and modulus of elasticity by 20% and 36%, respectively, when using 10 HA+10 $BaTiO_3$+PCL+PLA compared with PLA [91]. After a year, Zehuan Wang et al. (2020) mixed Ag-coated PNN-PZT with PDMS polymer and then used the mix as inks in a 3D printer to make the intricate three-dimensional grid structures that are piezoelectric and flexible, as seen in Figure 18. Electromechanical property tests are examined. The results indicated that the grid complex shape has more flexibility than ceramic only and has d_{33}, ε_r, g_{33}, FOM, and V0 as 58, 16, 0.4, 23.2, and 0.55, respectively. This study demonstrates that a 3D-printed flexible ceramic-polymer composite could be used instead of fragile piezoceramics to change electrical energy into mechanical energy [92]. In the same year, Yushun Zeng et. al. employed additive manufacturing along with 3D printing technology in the field of ultrasonic devices with a new design named honeycomb based on absorbing sound waves and converting them into electrical energy. Approximately 70 wt.% of $BaTiO_3$ into UV resin. After printing samples, they carried out some post-processes consisting of debinding and sintering, as illustrated in Figure 22. The result showed a high piezoelectric coefficient, which was 60 pc/n, and the voltage output reached 180 V_{opp} [86]. Finally, Zeyu Chen et. al. (2016) demonstrate that a piezoelectric-composite slurry with $BaTiO_3$ nanoparticles can be 3D printed using Mask-Image-Projection-based Stereolithography (MIP-SL) technology. After a post-process, the printed samples exhibit d_{33} and relative permittivity of 160 pCN^{-1} and 1350, respectively [93]. For a comprehensive comparison of the materials, particle sizes, additive percentages, and fabrication methods discussed in these summaries (Figure 23), refer to Table 5.

Hybrid system

The goal of a hybrid system is to increase the output voltage by combining other effects with the piezoelectric effect, such as the triboelectric effect or magnetic effects. It is also meant to improve the functionality of the device or tool by using the effects together, such as the shape memory effect in the scaffold field with the piezoelectric effect. The doctor uses the first to address irregular shapes in

Figure 21. LCD-SLA 3D printing of BT/UV samples [90]

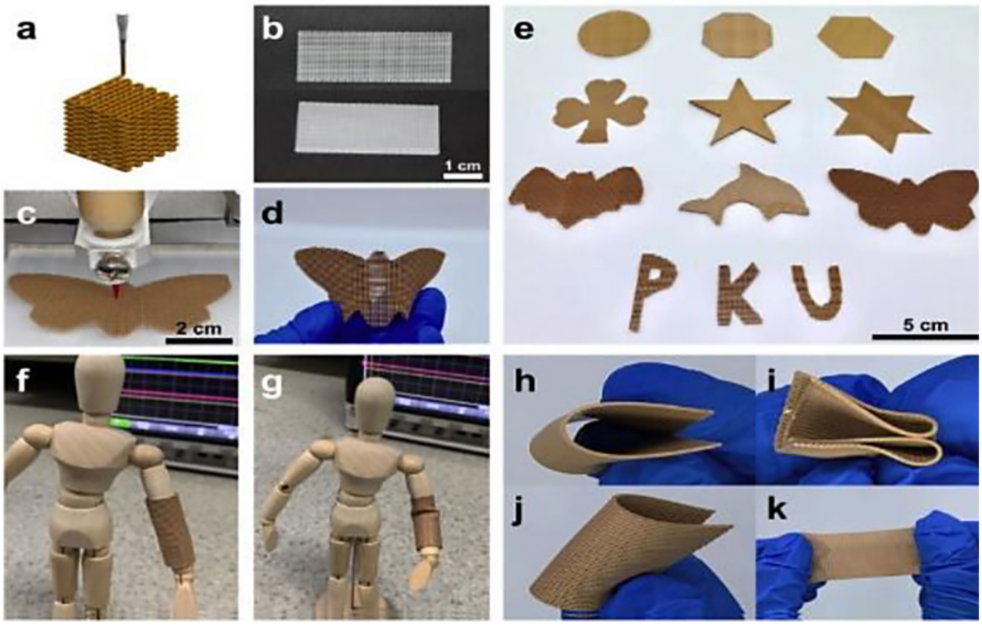

Figure 22. (a) Schematic illustration of 3D printing, (b) optical image of printed pure PDMS, (c–e) optical images of printed ceramic composites, (f, g) wearable printed material on a wooden doll before and after arm bending, (h–k) flexibility and stretching of printed composite presented by bending, twisting, and stretching [92]

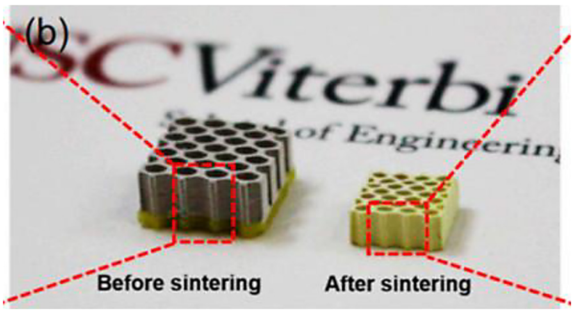

Figure 23. Size comparison of the samples before and after sintering [86]

bone defects, while the second enhances growth and healing. To begin with, Guanlin Li (2023), using an acrylate epoxidized soybean oil (AESO) matrix polymer doped with modified piezoelectric Ag-TMSPM-pBT (ATP), was prepared via 3D printing based on digital light processing to fabricate a multifunctional scaffold as illustrated in Figure 24. The 10 wt.% Ag-TMSPM-pBT + AESO scaffold exhibits promising piezoelectric properties, with a piezoelectric coefficient (d_{33}) of 0.9 pC N^{-1} and an output current of 146.4 nA, which are close to the piezoelectric constants of bone tissue. Moreover, these scaffolds exhibit a strong shape memory function and can quickly recover their original shape under near-infrared (NIR) light irradiation [95]. Subsequently, Hairong Chen et al. (2018) included the addition of PZT to SMP (PU) to fabricate an actuator using the solution casting method. The results indicated that the addition of PZT particles increased recovery stresses by 4.3 times at 80% and decreased recovery rate values. Despite this, the recovery rates are still no less than 94.5%. Additionally, it showed an enhancement in the tip displacement, which was measured by the displacement measurement system as illustrated in Figure 25 [96]. Furthering this exploration, Guoquan Suo et. al. (2016) incorporated $BaTiO_3$ nanoparticles into a PDMS matrix polymer to fabricate a piezoelectric film as illustrated in Figure 26 by the solution casting method. The device with 20% BTO in PDMS and a 100-µm-thick film showed the highest output power, while the hybrid output performance was higher than the tribo or piezoelectric performances [97]. Moving forward, a study presented by Zakharov et. al. proposes an enhanced method for thermal energy harvesting, exploiting combined pyroelectric, piezoelectric, and shape memory (SME) effects. A material that is pyroelectric is also piezoelectric. If it is combined with a material with SME by laminated structure as illustrated in the Figure 27, which generates large strain and stress in a rather narrow temperature range, the resulting laminated structure would generate voltage from temperature variations using two different energy conversion principles at once: (1) pyroelectric effect and (2)

Table 5. Summary of materials, particle size, enhancement methods, additive percentages, and fabrication approaches for piezoelectric 3D printing

No.	Year	Materials						Methods Enhancement	Add. %	Ref.
		Polymer Matrix Materials	Additive Materials	Particle Size	Electrode	Additive Layer	Modified Materials			
1.	2020	Photo curable UV resin	$BaTiO_3$	Nano size	Au/Cr	Epoxy for filling the Blank in the honeycomb	no	Additive manufacturing (DLP printer)+complex shape Metamaterials	50–70 wt.% were mixed with 30 – 50 wt. % photo curable resin	[86]
2.	2024	PHB	$BaTiO_3$	Nano size particle size < 3.0 μm	No	No	no	3d printer y FDM From powder to filament manufacture	0–20 wt.%	[87]
3.	2024	UV resin 35 – 55 wt. % + PVDF 20–40 wt. %	BN (boron nitride)	Nano tubes	Aluminum	No	(DEF) solvent 23% + HDODA 0.1% + BAPO 1.9%	3d printer SLA	2 wt.%	[88]
4.	2021	Deionized water	PZT	0.5 μm	Silver paint	No	No	Extrusion method with post- processing + die pressing method	11, 12.5, and 14 wt.% for water	[89]
5.	2021	Photo curable resin (SG15 resin)	$BaTiO_3$	Micron d_{50} = 3.4 μm d_{50} = 1.02 μm d_{50} = 50–70 nm	Silver-paste	No	No	3d printer LCD-SLA	70.1 wt.% (30 vol.%) and then less for nano to (20 vol.%)	[90]
6.	2020	PDMS	Ag-coated PNN-PZT + MWCNTs	Nano size	Undefined	No	AG coated Ceramic powder	3d inks printer	40 wt.% + 1 wt.% MW-CNTs	[92]
7.	2021	PLA PLA+PCL	HA HA+$BaTiO_3$	$BaTiO_3$ < 2 μm	No	No	Dichloromethane solvant	3d printer filaments (FDM) Hybrid material Hybrid functional	0-20 wt.%	[91]
8.	2016	Photo curable resin SI500	$BaTiO_3$	100 nm	Cr/Au	Conductive epoxy	Azeotropic mixture with dispersant	Additive manufacturing (DLP printer)+complex shape Met materials	70wt.%	[93]
9.	2015	Binding agent	$BaTiO_3$	0.85 to 1.45 μm	Silver paint	No	No	binder jetting additive manufacturing prior process and post process consistency of heat powder,debinding and sintering	Undefined	[94]

piezoelectric effect driven by SME. The results revealed that enhancement in voltage generation was 50% compared with the pyroelectric effect [98]. Applying a similar approach, Dong Cao et al. (2021) look into how to deposit a thin multilayer of P(VDF-TrFE) piezoelectric polymer on the NiTi SMA surface using the electrospinning method, as illustrated in the Figure 28. They want to make simple, scalable devices that can collect both mechanical and thermal energy. from the results that showed the d_{33} value was found to be 22.8 pC/N [99]. Expanding on this concept, Lilian Nunes et. al. (2024) propose a novel approach for the fabrication of magnetoelectric composites aimed at enhancing cross-coupling between electrical and magnetic phases for potential applications in intelligent sensors and electronic components. They used PZT fibers, cobalt ($CoFe_2O_4$), and a polymeric resin to make the composites as illustrated in Figure 29. According to SEM scans, the PZT-5A fibers were evenly distributed in the cobalt matrix. Dielectric measurements indicate stable behaviors, particularly when PZT-5A fibers are properly poled, showcasing potential applications in sensors or medical devices [100]. For a comprehensive comparison of the materials,

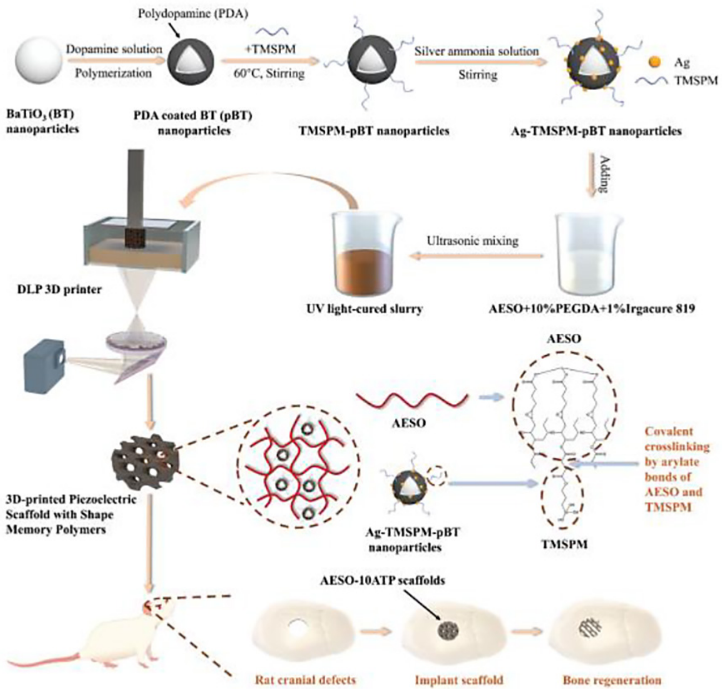

Figure 24. The preparation process of the Ag-TMSPM-pBT nanoparticles and the AESO scaffolds, and application of the AESO-10ATP scaffolds in bone regeneration [95]

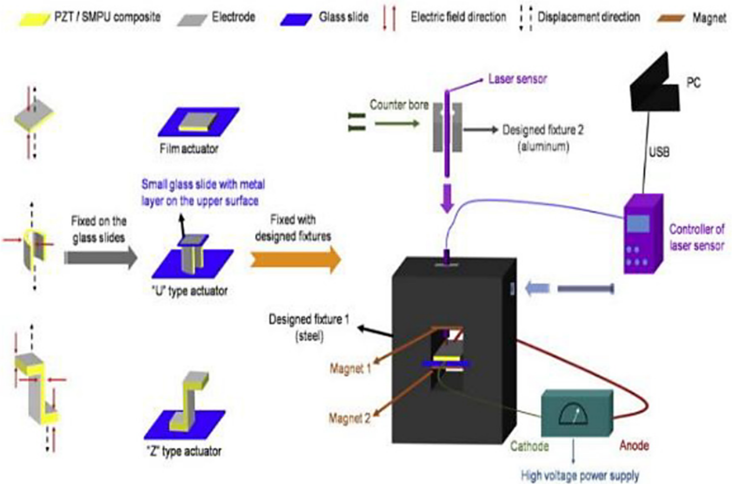

Figure 25. Schematic illustration of the displacement measurement system in a common experimental environment [96]

particle sizes, additive percentages, and fabrication methods discussed in these summaries, refer to Table 6.

Functionally graded materials system (FGMS)

At first, in the research published in 2022 by X.L. Yu et al., a theoretical study was included on the effect of the volume fraction of carbon nanotube and its distribution pattern on the natural frequency value. The volume fraction and distribution type of the CNT significantly affect the stiffness of the piezoelectric-integrated FG-CNTRC plate. As the CNT volume fraction increases, the natural frequency of the piezoelectric-integrated FG-CNTRC plate also increases. Additionally, the natural frequency of the piezoelectric FG-X CNTRC plate is relatively larger compared to other CNT distribution types, including UD, FG-O, and FG-V, as illustrated in the Figure 30 [101]. Furthering this research, in 2015, Satyanarayan et al. conducted a theoretical study

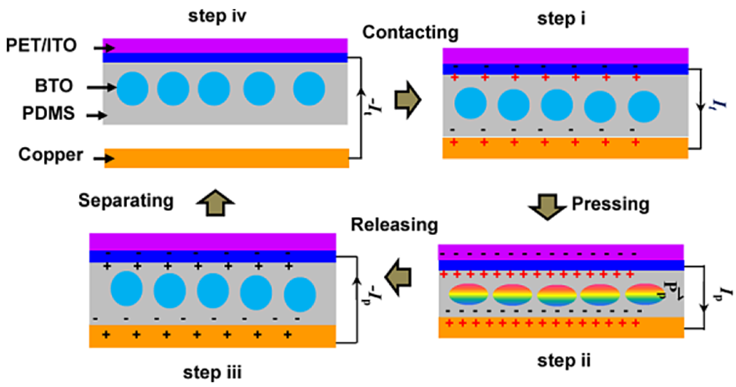

Figure 26. Stepwise operation mechanism used to investigate the combined effects of piezoelectricity and triboelectricity [97]

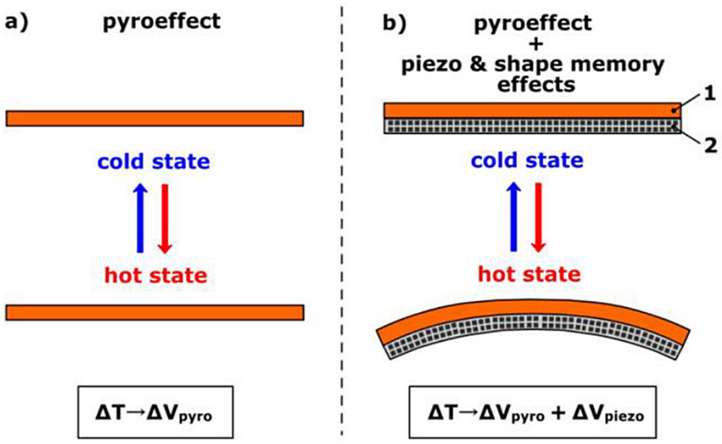

Figure 27. Principle of proposed enhancement of pyroelectric material performance. 1 – pyro/piezo-electric layer, 2 – SMA layer with SME pre-determined at the temperature range of interest [98]

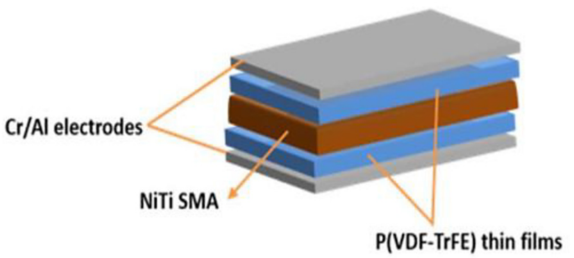

Figure 28. SMA/P(VDF-TrFE) multilayer composite structure [99]

by using functionally graded piezoelectric material PZT-Pt, as illustrated in Figure 31, to fabricate an actuator. The results showed an enhancement in frequency of 87.6%, which was 960 Hz as compared to the resonance frequency of 7761 Hz of the original design. The proposed functionally graded piezoelectric material actuator can be effectively used at low frequency (960 Hz) with high tip displacement (35 μm) under 500 V [102]. Furthering this research, in 2015, Satyanarayan et

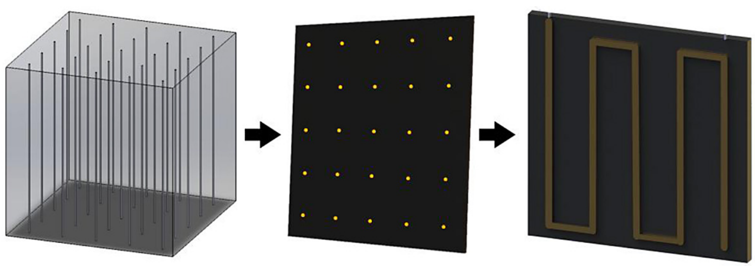

Figure 29. The cube composite, 1 mm-thick cuts perpendicular to the PZT-5A fibers, and the composite electrical connections (wiring schemes using silver ink to interconnect the PZT-5A fibers) [100]

Table 6. Summary of materials, particle size, enhancement methods, additive percentages, and fabrication approaches for piezoelectric hybrid systems

No.	Year	Materials						Methods Enhancement	Add. %	Ref.
		Polymer matrix materials	Additive materials	Particle size	Electrode	Additive layer	Modified materials			
1.	2017	PDMS	$BaTiO_3$	200 nm diameter	Cu	PET/ITO Layer upper and Cu and PET lower		Solvent casting Composite material New technique hybrid system	5–30 wt.%	[97]
2.	2018	PU (SMP)	PZT	400 nm	Pb-Pt alloy	No	Tetrahydrofuran (THF)	Combine Piezoelectric and shape memory effects Composite material Used solution casting and hot pressing	60, 70, 80 wt.%	[96]
3.	2023	AESO UV resin	$BaTiO_3$ (Ag-TMSPM-pBT)	Nano size	Copper	Kapton film	PDA + Ag + TMSPM	Combine Piezoelectric and shape memory effects hybrid material 3d printer SLA	5 10 20 wt.%	[95]
4.	2021	Ti-Ni-Cu (SMA)	Macro Fiber Composite	Un defined	Undefined	Undefined	No	Combine Piezoelectric , pyroelectric and SME effect Multilayer	undefined	[98]
5.	2021	PVDF-TrFE	NiTi SMA	Undefined	Cr/Al	No	No	Spin-coated multifunctional	layers	[99]
6.	2024	Polyester Resin	PZT fibers, cobalt ($CoFe_2O_4$)	Nano size	Silver ink	No		Solution casting and Fiber implant	undefined	[100]

al. conducted a theoretical study by using functionally graded piezoelectric material PZT-Pt, as illustrated in Figure 32, to fabricate an actuator. The results showed an enhancement in frequency of 87.6%, which was 960 Hz as compared to the resonance frequency of 7761 Hz of the original design. The proposed functionally graded piezoelectric material actuator can be effectively used at low frequency (960 Hz) with high tip displacement (35 µm) under 500 V [103].Continuing along these lines, In 2003, Kenta Takagi et. al. studied the effect of the functionally graded volume fraction of composition PZT/Pt on the mechanical, dielectric, piezoelectric, and elastic properties. Miniature bimorph-type FGM actuators that consist of a composite internal electrode (70 vol.% PZT/30 vol.% Pt) and three piezoelectric layers (100 vol.% PZT, 90 vol.% PZT/10 vol.% Pt, 80 vol.% PZT/20 vol.% Pt), as illustrated in the Figure 33, were fabricated by powder stacking and normal sintering techniques. The results showed an inverse relationship between the piezoelectric and dielectric properties and the amount of platinum, meaning that the more platinum there is in the composition, the lower the piezoelectric coefficient and dielectric constant values, despite the slight difference. Conversely, this relationship holds true for mechanical properties. especially the fracture toughness in the composites [104]. Finally, Abdulhakim Almajid et al. (2002) used a porous FGM system that consists of multiporous piezoelectric layers where the porosity gradient increases in the thickness direction. The porous FGM actuator is fabricated by co-sintering powder compacts of PZT and stearic acid in air. The electroelastic properties of each layer in the FGM systems were measured and used as input data in the analytical model to predict the FGM actuator curvature. The analytical predictions are found to agree well with the experimental measurements [105].

Coating techniques

Bio-piezoelectric materials were capable of improving the osseointegration properties of implants by converting mechanical forces into electrical signals that provided microelectrical stimulation for the formation and remodeling of bone tissue. Although metallic bioimplant materials can provide adequate mechanical strength, their surfaces were biologically inert as well as lacking the piezoelectric properties to stimulate osteogenesis.Xiaohui Sun et al. (2024) study coating zirconium alloys with deposition of $BaTiO_3$–$SrZrTiO_3$ piezoelectric material by magnetron sputtering to enhance osseointegration with the bone. The morphology and electrical properties were characterized. The results of the tests

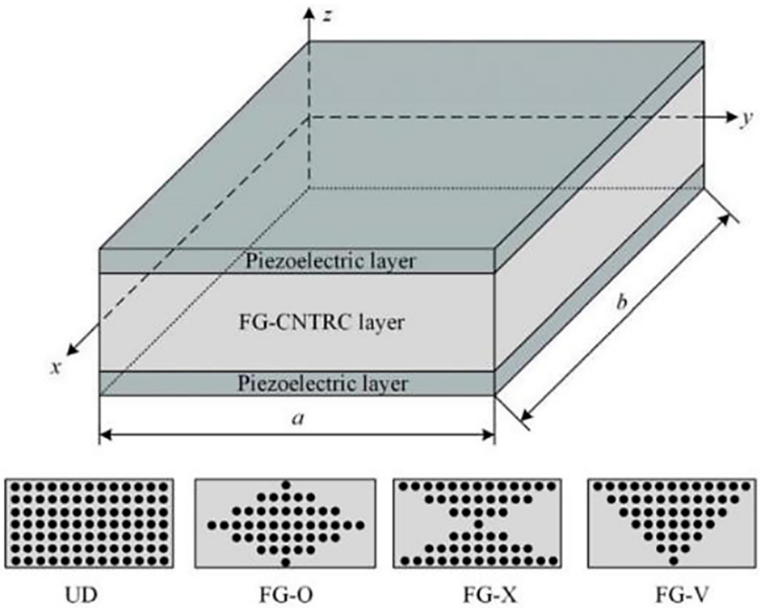

Figure 30. Configuration of the rectangular FG CNTRC plate with piezoelectric layers

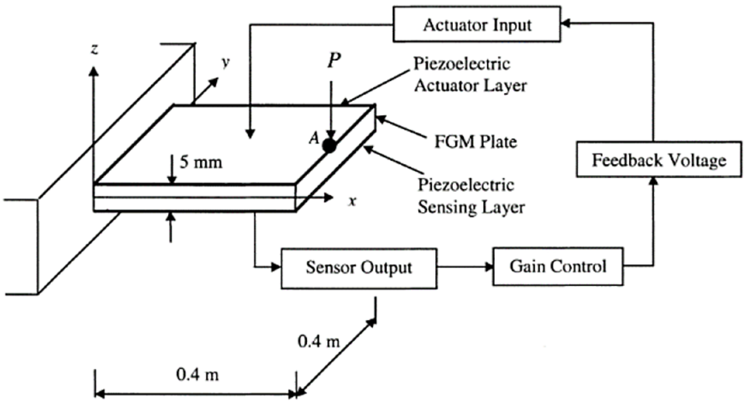

Figure 31. Schematic diagram showing the feedback configuration of the FGM plate with piezoelectric sensor/ actuator layers [102]

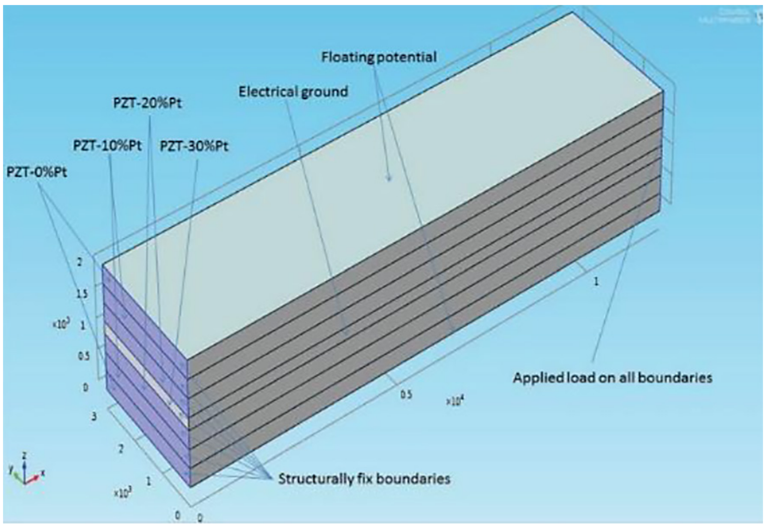

Figure 32. Schematic design of FGM cantilever actuator [103]

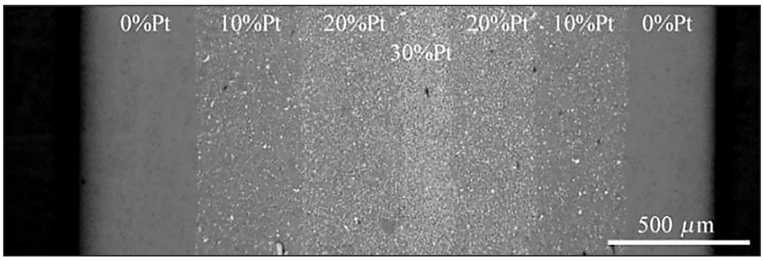

Figure 33. Optical microscopic photograph of the cross-section of PZT/Pt FGM bimorph actuator. The Pt volume fractions are indicated in the photograph [104]

indicated that the piezoelectric constant value was 5.02 pC/N for the zirconium alloy coating, which approximated the piezoelectric properties of natural bone tissue. Biological experiments indicated that the $BaTiO_3$–$SrZrTiO_3$ piezoelectric coated film had a good promotion effect on the early adhesion, proliferation, and differentiation of osteoblasts.[106]. Expanding on this approach, in 2021, Oriol Careta et al. published research on a Ti-based alloy that had been covered with piezoelectric zinc oxide (ZnO) in two different forms, a flat dense film and an array of nanosheets, as illustrated in Figure 34. The goal was to get cells to stimulate their own electrical activity. Researchers examined the coating's effect on proliferation, cell adhesion, differentiation marker expression, and the induction of calcium transients. The findings showed that ZnO nanosheets could only cause calcium fluctuations, which helped Saos-2 cells multiply and increased the expression of some genes involved in early differentiation. The normal movement of the cells puts stress on the ZnO nanosheets. These, in turn, create electric fields nearby because they are piezoelectric. These electric fields cause the opening of calcium voltage gates and boost cell proliferation and early differentiation [107]. Similarly, using the same principle but using a composite material from zinc oxide (ZnO) and titanium dioxide (TiO_2) with a particle size of 100 nm to coat the titanium substrate. Shumin Pang et al. (2019) studied the aim of fabricating a multifunctional coating. The results showed an enhancement in antibacterial, biocompatibility, and piezoelectric properties due to the coating process [108]. Taking this research a step further, Rui Zhou et al. (2019) study coating Ti substrate by bi-layered SnO_2–TiO_2 as illustrated in Figure 35. The crystallization of the TiO_2 interlayer facilitates the growth of SnO_2 nanorods, showing excellent hydrophilicity and good apatite-inducing ability due to the formation of a heterojunction. The results show a significant improvement in bonding strength with surrounding bone tissue, which makes it a suitable material for bone tissue replacement and repair [109].

HIGHLIGHTED POINTS

1) There are three methods for converting mechanical energy into the electrical energy needed by electronic devices: electromagnetic [23–26], electrostatic, and piezoelectric effects. Piezoelectric materials outperform electromagnetic and electrostatic methods due to their high energy conversion performance and high piezoelectric sensitivity. PEHs are robust and consistent, and

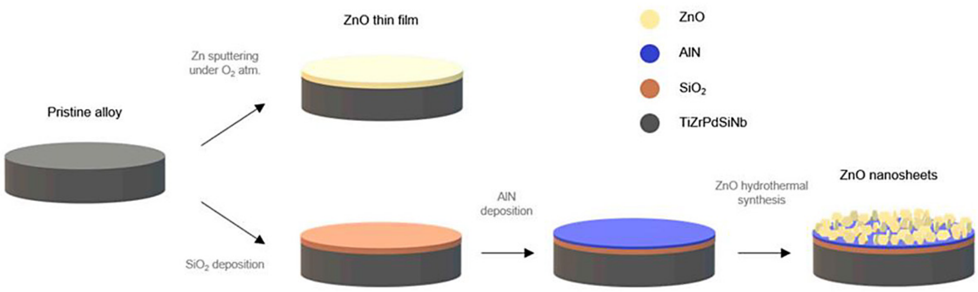

Figure 34. Schematic illustration of the coating process to obtain ZnO thin films (sputtering) and ZnO nanosheets (hydrothermal synthesis) on TiZrPdSiNb alloy [107]

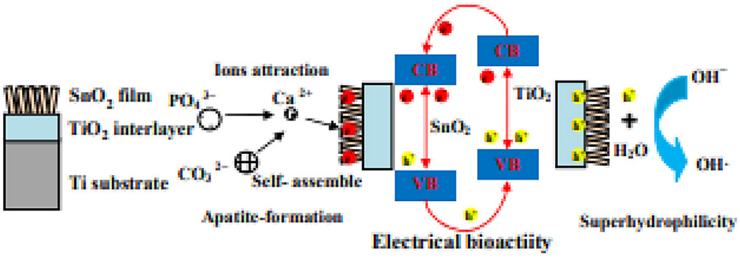

Figure 35. SnO_2-TiO_2 surface with the bi-layered structure on Ti provides internal electric stimulation to promote osteointegration of implant [109]

they are not impacted by external conditions such as humidity [1].

2) There are many different methods for enhancing properties of piezoelectric materials: composite and hybrid materials, partial size, shape, and dimension, compressibility, lamination, 3D printing, coating, functional grid materials, and hybrid systems, and each method is used to enhance one or more of the properties, for example, enhanced electromechanical coupling factor, piezoelectric coefficient, dielectric constant, flexibility, stretchability, toughness, and thermal conductivity. It is possible to combine more than one enhancement method to increase the functional efficiency of piezoelectricity and integrability for diverse applications.
3) There are several traditional methods to fabricate bulk piezoelectric ceramics (solution casting method, electrospinning (liquid), hot pressing (powder), biologically modified woodland, and spin-casting); however, most of those methods have restrictions regarding being able to produce a functional and complex shape for specific application needs [74] 3D printers can make piezoelectric ceramics with high solid addition with complex geometries and great material properties. These can then be used to make sensors, capacitors, and energy storage devices that are very specific to the user's needs. But it needs post-manufacturing processes, such as debinding and sintering processes for removing the resin or binder material, for example, to obtain dense samples [110]. AM has many advantages, such as low cost, multi-material parts, electromechanical response, piezoelectric constant, and size and shape [1]. 3D printing allows for the precise control of the material's composition, microstructure, and shape, which can significantly enhance piezoelectric materials' performance [49].
4) Representative piezoelectric materials can be categorized into piezoceramics, piezopolymers, and piezocomposites. Piezoceramics have large electro-mechanical coupling constants and provide a high energy conversion rate, but they are too brittle to use as general shape energy transducers. On the other hand, piezopolymers have smaller electromechanical coupling constants compared to the piezoceramics, but they are very flexible [32]. An example of this, $Pb(Zr,Ti)O_3$ (PZT)-based ceramics have excellent electromechanical energy conversion ability; however, their rigid and unreformed characters are not suitable for flexible electronics applications. To solve this problem, we use the principle of additive manufacturing, for example, a composite material of PDMS and PZT to form a flexible piezoelectric [92].
5) There are two types of piezoceramics: lead-based and lead-free [2]. Lead-containing piezoelectric materials typically show the highest energy conversion efficiencies, but due to their toxicity, they will be limited in future applications. In their bulk form, the piezoelectric properties of lead-free piezoelectric materials are significantly lower than those of lead-containing materials. However, the piezoelectric properties of lead-free piezoelectric materials at the nanoscale can be significantly larger than the bulk scale [45].
6) There are four types of materials that were looked at in this study: polymeric materials (like PVDF, PVDF-TrFE, and AESO UV resin), matrixes for ceramic additive powders (like PDMS, epoxy, PHB, PU, and photocurable UV resin), and binding agents (like Binding Agent 3D printer). The purpose of binding agents is to make the composite more flexible or to hold it together. Following its creation, the composite undergoes debinding and sintering processes to eliminate the binding agents. There are many

different types of additive filler reinforcement ceramic materials. Some of them are piezoelectric, like PZT, $BaTiO_3$, BN, KNN, $NaNbO_3$, RGO, $BiFeO_3$, ZF, $NaNbO_3$, and MnO_2. Other types, such as MWCNTs, SiC, glass fiber fabric, and HA, were added to improve mechanical, bioactive, electrical, and thermal conductivity. They were also laminated to improve mechanical properties, such as CFRP and GFRP. We add assistance materials to help mix the powders evenly within the matrix and prevent them from aggregating. Examples of these materials include UP-105 titanate coupling, SDS, N,N-dimethylformamide (DMF), PEG-6000, dispersant BYK, TMSPM, PA, and AG coating.

7) According to research on the sizes of the additives, mostly nanomaterials, the piezoelectric properties of nano are better than micro. However, when the ratios get high (70 wt.%), the micro materials' properties become better, and the nanoscale materials' piezoelectric response doesn't respond. This is explain in the research from Bharathi Ponraj et al. (2016). Furthermore, there is an inverse relationship between the submicron size and viscosity properties. The smaller the size, the higher the viscosity, and thus it will cause difficulty in the process of printing samples in the field of 3D printing, for example [77].
8) Poling is an essential step after piezoelectric device fabrication. It involves aligning the molecular dipoles in a single global direction within a structure by applying a high electric field. Poling is mainly performed in two ways: corona and thermal poling [1].
9) The efficiency of converting energy by using a piezoelectric device from one form to another is poor, and according to equation (η = output electrical energy/input mechanical energy), the results indicated that efficiency was 0.01546% by using a 3-point bending test [81].
10) The application of piezoelectricity to energy harvesting: Piezoelectric shoes [4], piezoelectric, pyroelectric, and ferroelectric-based sensors [61], utilized for powering microwatt power-consuming sensor devices [60], light-emitting diodes (LEDs) and charge capacitors [63], and micro devices for human energy harvesting for wearable biosensors [39], ultrasonic transducers [111], aviation radio equipment; in the marine industry for transceiver modules of hydroacoustic antennas; and in the nuclear industry for pressure control sensors in the steam–water path [90], soft robotics, artificial muscles, and biology signal identification [26], ultrasonic devices [86], sonar, or in medical ultrasonic devices [112], Wearable products, Hearing aid system, deep brain-stimulation system, retinal electrical stimulation system, pacemaker, and wheel pressure sensors [1], A magnetically coupled bistable piezoelectric energy harvesting structure for underwater applications [113], a piezoelectric rain energy harvester using a self-release tank [114], a rotating ring piezoelectric power generator [115], a tunable broadband piezoelectric harvester for ultralow-frequency bridge vibration energy harvesting [116], a floating ocean wave energy harvester coupled with piezoelectric material [116], a shock absorber [117], and a seismocardiography (SCG) sensor [76]. but has also been explored in other fields like micro-actuation systems (microfluidic chips) [59], active scaffolds [87], piezoelectric shape memory polymer scaffolds [95], and active adhesion implants [109].
11) One of the future proposals from this review is to utilize smart materials in conjunction with the 3D printer's multi-layer printing capability to produce multi-functional piezoelectric samples.
12) MWCNT can improve piezoelectric materials with a small addition ratio (0.5 wt.%) using the hybrid composition principle [67]. In addition, it improves the mechanical and thermal properties of the material. Since this is the case, it is considered a strong candidate for use in filler reinforcement in the field, combining piezoelectric and shape memory effects (hybrid system).
13) The piezoelectric performance typically undergoes several tests. These include looking at the material's physical and microstructure, mechanical and thermal properties, biocompatibility and biodegradation, and electrical, ferroelectric, and piezoelectric properties.

CONCLUSIONS

The studies looked at published work in the area of piezoelectricity and put it into groups based on the techniques used to enhance properties. These groups were made up of composite and hybrid materials, partial size, shape, and dimension, compressibility, lamination, 3D printed piezoelectric, coating, functional grid materials, and hybrid systems. For each method, different materials were used to prepare the piezoelectric. These materials can be broken down into several groups, such as smart materials that have piezoelectric effects, reinforcement materials, matrix materials, materials that help with the distribution process, electrode materials, In addition, we defined the size of the added materials, mostly nanomaterials. We can use this study to select materials, their specifications, and the improvement method. The real benefit of employing the review study lies in the possibility of integrating multiple improvement methods in a single future study. For instance, the study can be used to improve the hybrid system by using the hybrid composition method and piezoelectric surface particle shape (2-dimensional particle) supported by material fiber (1-dimensional particle) to improve the thermal and electrical conductivity. A 3D printer can manufacture the system due to its ability to create complex shapes. When choosing two- or one-dimensional additives, the goal is to keep the particles suspended in the mixture for as long as possible and keep the additives from agglomerating into the bottom of the printing vat during printing. This is one of the most important things to keep in mind, and you should test this type of piezoelectric particle additive material.

REFERENCES

1. Megdich, A., Habibi, M. and Laperrière, L. A review on 3D printed piezoelectric energy harvesters: materials, 3D printing techniques, and applications. Materials Today Communications, 2023; 35: 105541.
2. Banerjee, S., Bairagi, S. and Ali, S.W. A critical review on lead-free hybrid materials for next generation piezoelectric energy harvesting and conversion. Ceramics International, 2021; 47(12): 16402–16421.
3. Chalasani, S. and Conrad, J.M. A survey of energy harvesting sources for embedded systems. in IEEE SoutheastCon 2008. 2008. IEEE.
4. Chen, J.-X., et al. Piezoelectric property enhancement of PZT/Poly (vinylidenefluoride-co-trifluoroethylene) hybrid films for flexible piezoelectric energy harvesters. ACS omega, 2021; 7(1): 793–803.
5. Li, S. and Lipson, H. Vertical-stalk flapping-leaf generator for wind energy harvesting. in Smart materials, adaptive structures and intelligent systems. 2009.
6. Weimer, M.A., Paing, T.S. and Zane, R.A. Remote area wind energy harvesting for low-power autonomous sensors. in 2006 37th IEEE Power Electronics Specialists Conference. 2006. IEEE.
7. Li, S., Yuan, J. and Lipson, H. Ambient wind energy harvesting using cross-flow fluttering. Journal of applied physics, 2011; 109(2).
8. Wang, K., et al., A comprehensive review of geothermal energy extraction and utilization in oilfields. Journal of Petroleum Science and Engineering, 2018; 168: 465–477.
9. Glassley, W.E. Geothermal energy: renewable energy and the environment. 2014; CRC press.
10. Østergaard, P.A. and Lund, H. A renewable energy system in Frederikshavn using low-temperature geothermal energy for district heating. Applied Energy, 2011; 88(2): 479–487.
11. Al-Qadami, E.H.H., Mustaffa, Z. and Al-Atroush, M.E. Evaluation of the pavement geothermal energy harvesting technologies towards sustainability and renewable energy. Energies, 2022; 15(3): 1201.
12. Yoon, E.-J. and Yu, C.-G. Power management circuits for self-powered systems based on micro-scale solar energy harvesting. International Journal of Electronics, 2016; 103(3): 516–529.
13. Raghunathan, V., et al. Design considerations for solar energy harvesting wireless embedded systems. in IPSN 2005. Fourth International Symposium on Information Processing in Sensor Networks, 2005. 2005. IEEE.
14. Abdin, Z., et al. Solar energy harvesting with the application of nanotechnology. Renewable and sustainable energy reviews, 2013; 26: 837–852.
15. Pobering, S. and Schwesinger, N. A novel hydropower harvesting device. in 2004 International Conference on MEMS, NANO and Smart Systems (ICMENS’04). 2004. IEEE.
16. Maas, J. and Graf, C. Dielectric elastomers for hydro power harvesting. Smart Materials and Structures, 2012; 21(6): 064006.
17. Vu, D.L., Le, C.D. and Ahn, K.K. Functionalized graphene oxide/polyvinylidene fluoride composite membrane acting as a triboelectric layer for hydropower energy harvesting. International Journal of Energy Research, 2022; 46(7): 9549–9559.
18. Jiang, D., et al. Water-solid triboelectric nanogenerators: An alternative means for harvesting hydropower. Renewable and Sustainable Energy Reviews, 2019; 115: 109366.
19. Field, C.B., Campbell, J.E. and Lobell, D.B. Biomass energy: the scale of the potential resource. Trends in ecology & evolution, 2008; 23(2): 65–72.
20. Ko, C.-H., et al. Carbon sequestration potential via energy harvesting from agricultural biomass residues in Mekong River basin, Southeast Asia. Renewable and Sustainable Energy Reviews, 2017; 68: 1051–1062.

21. Singh, R. and Setiawan, A.D. Biomass energy policies and strategies: Harvesting potential in India and Indonesia. Renewable and Sustainable Energy Reviews, 2013; 22: 332–345.
22. Abbas, D., et al. Guidelines for harvesting forest biomass for energy: A synthesis of environmental considerations. Biomass and Bioenergy, 2011; 35(11): 4538–4546.
23. Bijak, J., et al. A 2-dof kinematic chain analysis of a magnetic spring excited by vibration generator based on a neural network design for energy harvesting applications. Inventions, 2023; 8(1): 34.
24. Bijak, J., et al. Magnetic flux density analysis of magnetic spring in energy harvester by hall-effect sensors and 2d magnetostatic fe model. Journal of Magnetism and Magnetic Materials, 2023; 579: 170796.
25. Sciuto, G.L., et al. Deep learning model for magnetic flux density prediction in magnetic spring on the vibration generator. IEEE Access, 2024.
26. Sciuto, G.L., et al. Displacement and magnetic induction measurements of energy harvester system based on magnetic spring integrated in the electromagnetic vibration generator. Journal of Vibration Engineering & Technologies, 2024; 12(3): 3305–3320.
27. Challa, V.R., et al. A vibration energy harvesting device with bidirectional resonance frequency tunability. Smart Materials and Structures, 2008; 17(1): 015035.
28. Gammaitoni, L., Neri, I. and Vocca, H. Nonlinear oscillators for vibration energy harvesting. Applied Physics Letters, 2009; 94(16).
29. Zuo, L. and Tang, X. Large-scale vibration energy harvesting. Journal of intelligent material systems and structures, 2013; 24(11): 1405–1430.
30. Beeby, S.P., et al. A micro electromagnetic generator for vibration energy harvesting. Journal of Micromechanics and microengineering, 2007; 17(7): 1257.
31. Erturk, A., Hoffmann, J. and Inman, D.J. A piezomagnetoelastic structure for broadband vibration energy harvesting. Applied Physics Letters, 2009. 94(25).
32. Kim, H.S., Kim, J.-H. and Kim, J. A review of piezoelectric energy harvesting based on vibration. International journal of precision engineering and manufacturing, 2011; 12: 1129–1141.
33. Sodano, H.A., Inman, D.J. and Park, G. A review of power harvesting from vibration using piezoelectric materials. Shock and Vibration Digest, 2004; 36(3): 197–206.
34. Sodano, H.A., Park, G. and Inman, D. Estimation of electric charge output for piezoelectric energy harvesting. Strain, 2004; 40(2): 49–58.
35. Guan, M. and Liao, W. On the efficiencies of piezoelectric energy harvesting circuits towards storage devicevoltages. Smart Materials and Structures, 2007; 16(2): 498.
36. Mateu, L. and Moll, F. Review of energy harvesting techniques and applications for microelectronics. Microtechnologies for the New Millennium 2005; 5837: SPIE.
37. Mateu, L. and Moll, F. Review of energy harvesting techniques and applications for microelectronics. in VLSI Circuits and Systems II. 2005. SPIE.
38. Banerjee, S., Bairagi, S., & Ali, S. W. (2021). A critical review on lead-free hybrid materials for next generation piezoelectric energy harvesting and conversion. Ceramics International, 47(12), 16402–16421.
39. Sobianin, I., S.D. Psoma, and Tourlidakis, A. A 3D-printed piezoelectric microdevice for human energy harvesting for wearable biosensors. Micromachines, 2024; 15(1): 118.
40. Rayegani, A., et al. Recent advances in self-powered wearable sensors based on piezoelectric and triboelectric nanogenerators. Biosensors, 2022; 13(1): 37.
41. Mahanty, B., et al. All-fiber pyro-and piezo-electric nanogenerator for IoT based self-powered healthcare monitoring. Materials Advances, 2021; 2(13): 4370–4379.
42. Iqbal, M., et al. Multimodal hybrid piezoelectric-electromagnetic insole energy harvester using PVDF generators. Electronics, 2020; 9(4): 635.
43. Sezer, N. and Koç, M. A comprehensive review on the state-of-the-art of piezoelectric energy harvesting. Nano energy, 2021; 80: 105567.
44. Zhao, J., et al. A review of piezoelectric metamaterials for underwater equipment. Frontiers in Physics, 2022; 10: 1068838.
45. Bhadwal, N., Ben Mrad, R. and Behdinan, K. Review of zinc oxide piezoelectric nanogenerators: piezoelectric properties, composite structures and power output. Sensors, 2023; 23(8): 3859.
46. Sarker, M.R., et al. Review of piezoelectric energy harvesting system and application of optimization techniques to enhance the performance of the harvesting system. Sensors and Actuators A: Physical, 2019; 300: 111634.
47. Safaei, M., Sodano, H.A. and Anton, S.R. A review of energy harvesting using piezoelectric materials: state-of-the-art a decade later (2008–2018). Smart materials and structures, 2019; 28(11): 113001.
48. Wang, Q. and Wu, N. A review on structural enhancement and repair using piezoelectric materials and shape memory alloys. Smart Materials and Structures, 2011; 21(1): 013001.
49. Park, J., et al. A review on recent advances in piezoelectric ceramic 3D printing. in Actuators. 2023. MDPI.
50. Lee, D.-G.S., J.; Kim, H.S.; Hur, S.; Sun, S.; Jang, J.-S.; Chang, S.; Jung, I.; Nahm, S.; Kang, H.; et al. Autonomous ResonanceTuning Mechanism for Environmental Adaptive Energy Harvesting. Adv. Sci. 2023; 10, 2205179.

51. Briscoe, J.D., S. 2.1 Background. In Nanostructured Piezoelectric Energy Harvesters, 1st ed.; Springer and G. International Publishing: Berlin/Heidelberg, 2014; 3–4.
52. Erturk, A. and Inman, D. 1.4 Summary of the Theory of Linear Piezoelectricity. Piezoelectric Energy Harvesting, 1st ed.; John Wiley & Sons: Hoboken, NJ, USA, 2011: 9–12.
53. De Almeida, B.V. and Pavanello, R. Topology optimization of the thickness profile of bimorph piezoelectric energy harvesting devices. Journal of Applied and Computational Mechanics, 2019; 5(1): 113–127.
54. Holman, J.P. Experimental Methods for Engineers. 2012: McGraw-Hill/Connect Learn Succeed.
55. Covaci, C. and Gontean, A. Piezoelectric energy harvesting solutions: A review. Sensors, 2020; 20(12): 3512.
56. Lippmann, G. Principe de la conservation de l'électricité, ou second principe de la théorie des phénomènes électriques. J. Phys. Theor. Appl., 1881; 10(1): 381–394.
57. Koh, S.J.A., Zhao, X. and Suo, Z. Maximal energy that can be converted by a dielectric elastomer generator. Applied Physics Letters, 2009; 94(26).
58. Soin, N., Anand, S.C. and Shah, T.H. Energy harvesting and storage textiles, in Handbook of Technical Textiles. Woodhead Publishing. 2016; 357–396.
59. Zhang, C., Sun, H. and Zhu, Q. Preparation and property enhancement of poly (Vinylidene Fluoride) (PVDF)/lead zirconate titanate (PZT) composite piezoelectric films. Journal of Electronic Materials, 2021; 50: 6426–6437.
60. Chinya, I., Pal, A. and Sen, S. Polyglycolated zinc ferrite incorporated poly (vinylidene fluoride) (PVDF) composites with enhanced piezoelectric response. Journal of Alloys and Compounds, 2017; 722: 829–838.
61. Anand, A. and Bhatnagar, M. Effect of sodium niobate (NaNbO3) nanorods on β-phase enhancement in polyvinylidene fluoride (PVDF) polymer. Materials Research Express, 2019; 6(5): 055011.
62. Ganesh, R.S., et al. Microstructure, structural, optical and piezoelectric properties of BiFeO3 nanopowder synthesized from sol-gel. Current Applied Physics, 2017; 17(3): 409–416.
63. Ren, X., et al. Flexible lead-free BiFeO3/PDMS-based nanogenerator as piezoelectric energy harvester. ACS applied materials & interfaces, 2016; 8(39): 26190–26197.
64. Wang, F., et al. High quality barium titanate nanofibers for flexible piezoelectric device applications. Sensors and Actuators A: Physical, 2015; 233: 195–201.
65. Wang, A., et al. Self-powered wearable pressure sensors with enhanced piezoelectric properties of aligned P (VDF-TrFE)/MWCNT composites for monitoring human physiological and muscle motion signs. Nanomaterials, 2018; 8(12): 1021.
66. Siddiqui, S., et al. High-performance flexible lead-free nanocomposite piezoelectric nanogenerator for biomechanical energy harvesting and storage. Nano Energy, 2015; 15: 177–185.
67. Shoorangiz, M., Sherafat, Z. and Bagherzadeh, E. CNT loaded PVDF-KNN nanocomposite films with enhanced piezoelectric properties. Ceramics International, 2022; 48(11): 15180–15188.
68. Bairagi, S. and Ali, S.W. Investigating the role of carbon nanotubes (CNTs) in the piezoelectric performance of a PVDF/KNN-based electrospun nanogenerator. Soft Matter, 2020; 16(20): 4876–4886.
69. Amoozegar, V., Sherafat, Z. and Bagherzadeh, E. Enhanced dielectric and piezoelectric properties in potassium sodium niobate/polyvinylidene fluoride composites using nano-silicon carbide as an additive. Ceramics International, 2021; 47(20): 28260–28267.
70. Maruyama, K., et al. Electromechanical characterization and kinetic energy harvesting of piezoelectric nanocomposites reinforced with glass fibers. Composites Science and Technology, 2022; 223: 109408.
71. Singh, H.H., Singh, S. and Khare, N. Design of flexible PVDF/NaNbO3/RGO nanogenerator and understanding the role of nanofillers in the output voltage signal. Composites Science and Technology, 2017; 149: 127–133.
72. Yan, J. and Jeong, Y.G. Roles of carbon nanotube and BaTiO3 nanofiber in the electrical, dielectric and piezoelectric properties of flexible nanocomposite generators. Composites Science and Technology, 2017; 144: 1–10.
73. Chen, X., et al. Effect of the particle size on the performance of BaTiO3 piezoelectric ceramics produced by additive manufacturing. Ceramics International, 2022; 48(1): 1285–1292.
74. Renteria, A., et al. Particle size influence on material properties of BaTiO3 ceramics fabricated using freeze-form extrusion 3D printing. Materials Research Express, 2019; 6(11): 115211.
75. Renteria, A., et al. Influence of bimodal particle distribution on material properties of BaTiO3 fabricated by paste extrusion 3D printing. Ceramics International, 2021; 47(13): 18477–18486.
76. Li, J.-W., et al. Enhanced piezoelectric properties of poly (vinylidenefluoride-co-trifluoroethylene)/carbon-based nanomaterial composite films for pressure sensing applications. Polymers, 2020; 12(12): 2999.
77. Ponraj, B., Bhimireddi, R. and Varma, K. Effect of nano-and micron-sized K 0.5 Na 0.5 NbO 3 fillers on the dielectric and piezoelectric properties of PVDF composites. Journal of Advanced Ceramics, 2016; 5: 308–320.

78. Sun, J., et al. Enhanced mechanical energy conversion with selectively decayed wood. Science Advances, 2021; 7(11): eabd9138.
79. Sun, J., et al. Sustainable and biodegradable wood sponge piezoelectric nanogenerator for sensing and energy harvesting applications. ACS nano, 2020; 14(11): 14665–14674.
80. Yu, Y., et al. Carbon Fiber-Reinforced Piezoelectric Nanocomposites: Design, Fabrication and Evaluation for Damage Detection and Energy Harvesting. Composites Part A: Applied Science and Manufacturing, 2023; 172: 107587.
81. Yu, Y. and Narita, F. Evaluation of electromechanical properties and conversion efficiency of piezoelectric nanocomposites with carbon-fiber-reinforced polymer electrodes for stress sensing and energy harvesting. Polymers, 2021; 13(18): 3184.
82. Wang, Z., et al. Potassium sodium niobate lead-free piezoelectric nanocomposite generators based on carbon-fiber-reinforced polymer electrodes for energy-harvesting structures. Composites Science and Technology, 2020; 199: 108331.
83. Kurita, H., et al. Fabrication and mechanical properties of carbon-fiber-reinforced polymer composites with lead-free piezoelectric nanoparticles. Sens. Mater, 2020; 32(7).
84. Narita, F., Nagaoka, H. and Wang, Z. Fabrication and impact output voltage characteristics of carbon fiber reinforced polymer composites with lead-free piezoelectric nano-particles. Materials Letters, 2019; 236: 487–490.
85. Tien, C.M.T. and Goo, N.S. Use of a piezocomposite generating element in energy harvesting. Journal of Intelligent Material Systems and Structures, 2010; 21(14): 1427–1436.
86. Zeng, Y., et al. 3D-printing piezoelectric composite with honeycomb structure for ultrasonic devices. Micromachines, 2020; 11(8): 713.
87. Strangis, G., et al. 3D Printed Piezoelectric BaTiO3/Polyhydroxybutyrate Nanocomposite Scaffolds for Bone Tissue Engineering. Bioengineering, 2024; 11(2): 193.
88. Srinivasaraghavan Govindarajan, R., et al. Polymer nanocomposite sensors with improved piezoelectric properties through additive manufacturing. Sensors, 2024; 24(9): 2694.
89. Hall, S.E., et al. Paste extrusion 3D printing and characterization of lead zirconate titanate piezoelectric ceramics. Ceramics International, 2021; 47(15): 22042–22048.
90. Sotov, A., et al. LCD-SLA 3D printing of BaTiO3 piezoelectric ceramics. Ceramics International, 2021; 47(21): 30358-30366.
91. Mystiridou, E., Patsidis, A.C. and Bouropoulos, N. Development and characterization of 3D printed multifunctional bioscaffolds based on PLA/PCL/HAp/BaTiO3 composites. Applied Sciences, 2021; 11(9): 4253.
92. Wang, Z., et al. 3D-printed flexible, Ag-coated PNN-PZT ceramic-polymer grid-composite for electromechanical energy conversion. Nano Energy, 2020; 73: 104737.
93. Chen, Z., et al. 3D printing of piezoelectric element for energy focusing and ultrasonic sensing. Nano Energy, 2016; 27: 78–86.
94. Gaytan, S., et al. Fabrication of barium titanate by binder jetting additive manufacturing technology. Ceramics International, 2015; 41(5): 6610–6619.
95. Li, G., et al. 3D-Printed Piezoelectric Scaffolds with Shape Memory Polymer for Bone Regeneration. Small, 2023; 19(40): 2302927.
96. Chen, H., et al. Smart composites of piezoelectric particles and shape memory polymers for actuation and nanopositioning. Composites Science and Technology, 2018; 163: 123–132.
97. Suo, G., et al. Piezoelectric and triboelectric dual effects in mechanical-energy harvesting using BaTiO3/polydimethylsiloxane composite film. ACS applied materials & interfaces, 2016; 8(50): 34335–34341.
98. Zakharov, D., et al. Combined pyroelectric, piezoelectric and shape memory effects for thermal energy harvesting. in Journal of Physics: Conference Series. 2013. IOP Publishing.
99. Sukumaran, S. Design and preparation of a micro-harvesting device made of hybrid SMA/Piezoelectric polymer composite. 2021, Université de Lorraine.
100. Pereira, L.N., et al. Designing Multifunctional Multiferroic Composites for Advanced Electronic Applications. Electronics, 2024; 13(12): 2266.
101. Yu, X., Zhang, X. and Wang, J. Active vibration control of functionally graded carbon nanotube reinforced composite plate with coupled electromechanical actuation. Frontiers in Materials, 2022; 9: 861388.
102. He, X., et al. Active control of FGM plates with integrated piezoelectric sensors and actuators. International journal of Solids and Structures, 2001; 38(9): 1641–1655.
103. Patel, S. and Vaish, R. Design of PZT–Pt functionally graded piezoelectric material for low-frequency actuation applications. Journal of Intelligent Material Systems and Structures, 2015; 26(3): 321–327.
104. Takagi, K., et al. Fabrication and evaluation of PZT/Pt piezoelectric composites and functionally graded actuators. Journal of the European Ceramic Society, 2003; 23(10): 1577–1583.
105. Almajid, A., et al. Fabrication and modeling of porous FGM piezoelectric actuators. in Smart Structures and Materials 2002: Smart Structures

and Integrated Systems. 2002. SPIE.
106. Sun, X., et al. Enhanced biocompatibility and osseointegration properties of magnetron sputtered BTO-SZTO bio-piezoelectrically coated films as zirconium alloy implants. Materials Chemistry and Physics, 2024; 311: 128545.
107. Careta, O., et al. ZnO nanosheet-coated TiZrPdSiNb alloy as a piezoelectric hybrid material for self-stimulating orthopedic implants. Biomedicines, 2021; 9(4): 352.
108. Pang, S., et al. Multifunctional ZnO/TiO2 nanoarray composite coating with antibacterial activity, cytocompatibility and piezoelectricity. Ceramics International, 2019; 45(10): 12663–12671.
109. Zhou, R., et al. Electrically bioactive coating on Ti with bi-layered SnO 2–TiO 2 hetero-structure for improving osteointegration. Journal of Materials Chemistry B, 2018; 6(23): 3989–3998.
110. Renteria, A., et al. Optimization of 3D printing parameters for BaTiO3 piezoelectric ceramics through design of experiments. Materials Research Express, 2019; 6(8): 085706.
111. Zheng, K., et al. 3D printed piezoelectric focused element for ultrasonic transducer. Ceramics International, 2024.
112. Park, J., Lee, D. G., Hur, S., Baik, J. M., Kim, H. S., & Song, H. C. A Review on Recent Advances in Piezoelectric Ceramic 3D Printing. In Actuators 2023, April; 12(4), 177. MDPI.
113. Zou, H.-X., et al. A magnetically coupled bistable piezoelectric harvester for underwater energy harvesting. Energy, 2021; 217: 119429.
114. Bao, B. and Wang, Q. A rain energy harvester using a self-release tank. Mechanical Systems and Signal Processing, 2021; 147: 107099.
115. Xie, X., Wang, Q. and Wu, N. A ring piezoelectric energy harvester excited by magnetic forces. International Journal of Engineering Science, 2014; 77: 71–78.
116. Li, M. and Jing, X. Novel tunable broadband piezoelectric harvesters for ultralow-frequency bridge vibration energy harvesting. Applied Energy, 2019. 255: 113829.
117. Liu, M., Xu, J. and Li, Q. Design and experiment of piezoelectric-shape memory alloy composite shock absorber. Materials Letters, 2021; 304: 130538.